Carbon dioxide (CO_2) sorption to Na-rich montmorillonite at Carbon Capture, Utilization and Storage (CCUS) P-T conditions in saline formations

Elizabeth Gayle Krukowski

Thesis submitted to the faculty of the Virginia Polytechnic Institute and State University in partial fulfillment of the requirements for the degree of

Master of Science

In

Geosciences

Robert J. Bodnar

J. Donald Rimstidt

Nancy L. Ross

Gernot Rother

December 11th, 2012

Blacksburg, VA

Keywords: carbon dioxide, montmorillonite, carbon capture and sequestration, carbon capture utilization and sequestration, climate change, FTIR spectroscopy, smectite

© Elizabeth G. Krukowski, 2012

Carbon dioxide (CO_2) sorption to Na-rich montmorillonite at Carbon Capture, Utilization and Storage (CCUS) P-T conditions in saline formations

Elizabeth G. Krukowski

ABSTRACT

Carbon capture, utilization and storage (CCUS) in confined saline aquifers in sedimentary formations has the potential to reduce the impact of fossil fuel combustion on climate change by storing CO_2 in geologic formations in perpetuity. At PT conditions relevant to CCUS, CO_2 is less dense than the pre-existing brine in the formation, and the more buoyant CO_2 will migrate to the top of the formation where it will be in contact with cap rock. A typical cap rock is clay-rich shale, and interactions between shales and CO_2 are poorly understood at PT conditions appropriate for CCUS in saline formations. In this study, the interaction of CO_2 with clay minerals in the cap rock overlying a saline formation has been examined, using Na-rich montmorillonite as an analog for clay-rich shale. Attenuated Total Reflectance – Fourier Transform Infrared Spectroscopy (ATR -FTIR) was used to identify potential crystallographic sites (AlAlOH, AlMgOH and interlayer space) where CO_2 could interact with montmorillonite at 35°C and 50°C and from 0-1200 psi. Analysis of the data indicates that CO_2 that is preferentially incorporated into the interlayer space, with dehydrated montmorillonite capable of incorporating more CO_2 than hydrated montmorillonite. No evidence of chemical interactions between CO_2 and montmorillonite were identified, and no spectroscopic evidence for carbonate mineral formation was observed. Further work is needed to determine if reservoir seal quality is more likely to be degraded or enhanced by CO_2 - montmorillonite interactions.

ACKNOWLEDGMENTS

First and foremost I would like to thank Angela Goodman. Without her help and guidance, the FTIR experiments would not have been possible. She was always ready to answer any question and provide additional information that was useful. Her quick responses to emails and continuous encouraging support are greatly appreciated.

This thesis would not have been possible without support from my committee members, Robert J. Bodnar, J. Donald Rimstidt, Nancy Ross, and Gernot Rother. While their suggested changes were not always easy or straightforward, they greatly improved the quality of this research and challenged me as a scientist to do my best.

Additionally I would like to thank the Bodnar group of graduate students Ryan Capobianco, Pilar Lecumberri-Sanchez, Matthew Steele-MacInnis, Daniel Moncada, Hector LaMadrid, and Denise Levitan. Their quick response to questions and help along the way has been invaluable. Whenever I had a question about how to properly do something, I always knew I could ask any of them for help and they would do their best to answer my question.

I would also like to thank Kristie Dorfler and Ryan Capobianco for helping to keep me sane through this entire process. Kristie helped me to increase my productivity by being available for helpful chats to not just get through graduate school, but to look at our research in new and exciting ways. Ryan was always available to talk about new ideas and had helpful insights that allowed me to view my research in a new light. His humor and desire for me to succeed helped me get through many days that seemed rather dreary otherwise.

Last, but definitely not least I would like to thank my amazing family for their continual support. First among them being my wonderful husband, Daniel Krukowski. Even though I did not always talk about my research with him, he was always there for me at the end of the day whether it was good or bad. When I did talk about my research he always listened and gave useful suggestions to make it better. I know I can always count on him to support me through any endeavor I take on for the future. Thank you, Daniel! I would also like to thank my mother, Earlene VanDerel and my step-father, Joseph VanDerel, for their unwavering support throughout the entire process. Their constant love and helpfulness brightened up my days. Knowing they would always be there for me helped me to complete the program and will be a constant source of support throughout my life. Thank you Mom & Dad!

This research effort was partially performed in support of the National Energy Technology Laboratory under Contract DE-FE-0004000.

TABLE OF CONTENTS

ABSTRACT ……. ii

ACKNOWLEDGEMENTS……. iii

LIST OF FIGURES…… v-vi

1. **INTRODUCTION**…… 1
   - 1.1 Global Warming Background…… 1
   - 1.2 Study Objectives…… 4

2. **BACKGROUND**…… 6
   - 2.1 Smectite Background…… 6
   - 2.2 Montmorillonite Background…… 6
   - 2.3 Background Montmorillonite Studies…….. 7

3. **EXPERIMENTAL SETUP**…… 10
   - 3.1 ATR-FTIR Setup…….. 10
   - 3.2 Montmorillonite Sample…… 12
   - 3.3 FTIR Sample Preparation…….. 12
   - 3.4 Data Processing…….. 13

4. **RESULTS AND DISCUSSION**…….. 16
   - 4.1 Background Spectrum……16
   - 4.2 Pressure Test…… 18
   - 4.3 Equilibration Time…….19
   - 4.4 Peak Position and Peak Area Changes with CO_2 Pressure……21
   - 4.5 Temperature Effects…… 21
   - 4.6 Hydration Effects…….. 23
   - 4.7 Desorption Isotherms…… 27
   - 4.8 Residual CO_2 …… 27

5. **SUMMARY**…… 31

REFERENCES…… 32

APPENDIX A: Notebook Pages…….. 35-A

APPENDIX B: Raw and Subtracted Data…… 64-B

LIST OF FIGURES

Figure 1: Schematic representation depicting the injection of CO_2 emissions from a fossil fuel power plant into a saline formation beneath an impermeable shale cap rock ... 3

Figure 2: The crystallographic structure of montmorillonite viewed along [100]..……..…. 5

Figure 3: Schematic diagram of the ATR-FTIR cell setup …… 11

Figure 4: Representative FTIR spectra obtained in this study …… 14

Figure 5: FTIR spectrum of montmorillonite without CO_2 present in the cell…… 17

Figure 6: Comparison of the bands from the hydrated montmorillonite sample when exposed to N_2 and CO_2 atmosphere ..…… 19

Figure 7: Shown left is CO_2 v_3 antisymmetric stretch band at 2343 cm^{-1} and on the right is CO_2 v_2 bending mode at 659 cm^{-1} in the hydrated montmorillonite sample…… 20

Figure 8: The effect of time on the peak position and peak area for the v_3 CO_2, AlAlOH, and AlMgOH bands in the montmorillonite sample at 78 psi CO_2 pressure …… 20

Figure 9: The effect of CO_2 pressure on positions of v_3 CO_2, AlAlOH and AlMgOH peaks ……. 22

Figure 10: Comparison of increasing pressure effects versus peak area on v_3 CO_2, AlAlOH and AlMgOH …….. 22

Figure 11: Effect of temperature on peak positions …….. 23

Figure 12: Comparison of spectra of hydrated and dehydrated montmorillonite with no CO_2 present …… 24

Figure 13: Comparison of the spectrum of dehydrated montmorillonite in the absence of CO_2 and in the presence of CO_2…… 25

Figure 14: Comparison of the spectrum of re-hydrated montmorillonite in the absence of CO_2 and in the presence of CO_2…… 26

Figure 15: Peak position shift as a function of the amount of time that the sample is exposed to ~600 psi CO_2……..…… 28

Figure 16: Peak areas as a function of the amount of time that the sample is exposed to ~600 psi CO_2……..…… 28

Figure 17: Comparison of the peak area corresponding to nonstructural (interlayer) water (3400 cm^{-1}) in hydrated and dehydrated montmorillonite as a function of exposure time at ~600 psi CO_2.…… 29

Figure 18: Comparison of the area of the v_3 CO_2 peak under ~100 psi CO_2 pressure, and the area of this same peak after the pressure had been dropped to ~1 bar …… 29

1. INTRODUCTION

1.1 *Global Warming Background*

One of the most significant environmental challenges facing mankind today is climate change, or global warming (IPCC, 2005). Global warming occurs when greenhouse gases (GHG's) in the atmosphere trap radiant heat from the sun, resulting in warming of the atmosphere and the Earth's surface. Greenhouse gases include carbon dioxide (CO_2), methane (CH_4) and nitrous oxide (N_2O), as well as various chlorofluorocarbons (CFC's) and hydrochlorofluorocarbons (HCFC's) (IPCC, 2005). The process whereby GHG's trap heat and warm the Earth has been ongoing since the Earth was formed, and the regulating effect of GHG's has been critical to the origin, evolution and survival of life on Earth (Nisbet and Sleep, 2001). Atmospheric CO_2 has received the most scrutiny in the climate change discussion, and this gas has natural sources, including volcanic outgassing, decay and/or burning of vegetation, and respiration, as well as anthropogenic sources. The major anthropogenic source of CO_2 emissions is from the burning of fossil fuels, including coal, gasoline and natural gas. These CO_2 emissions can originate from a point source, such as an electric power-generating plant or a cement manufacturing plant, or from non-stationary sources such as automobiles and other forms of petroleum-based transportation. In recent years, there has been a significant increase in the concentration of CO_2 in the atmosphere that parallels recent increases in global average temperature, and evidence suggests that the increase in temperature is linked to the increase in atmospheric CO_2. And, while the overall and long-term impacts of climate change are uncertain, potential effects include loss of polar ice caps, rise in sea level, loss of habitat and reduced biodiversity, loss of cropland, increase in occurrence of some diseases such as malaria and dengue fever, and more common and severe extreme weather events (IPCC, 2005, 2012; Patz et

al., 1996). As a result, there has been much discussion concerning methods to reduce anthropogenic CO_2 emissions, and these range from overall energy conservation, to reducing our dependence on fossil fuels, to developing methodologies to reduce CO_2 emissions to the atmosphere from burning of fossil fuels.

Carbon capture, utilization and storage (CCUS) is a method whereby flue gas emitted from a stationary source such as a coal-fired power plant is captured and the CO_2 is stored or sequestered in a manner that prevents its introduction into the atmosphere (Greenwald, 2012; McConnell, 2012). One CCUS option that holds great promise involves the separation of CO_2 from the flue gas at the point of origin (i.e., a fossil-fuel-fired power plant), transport of the CO_2 as a supercritical phase to the point of injection, followed by injection into a subsurface geologic formation where it can be held permanently (Herzog, 2001). Geological formations that have been proposed for CCUS include deep, unmineable coal seams, depleted oil and gas reservoirs, organic-rich shales, basalts, and deep saline formations (Cygan et al., 2010).

One geological storage scenario that has received considerable attention is deep saline formations, owing to the enormous potential for CO_2 storage in this environment, with some storage capacity estimates as high as 20 billion metric tons of CO_2, representing about 450 years of storage at current production rates (Cygan et al., 2010). A requirement of any saline formation environment being considered for CCUS is that it must include a permeable horizon that can accommodate the large volumes of CO_2 that will be injected, as well as an impermeable confining layer to maintain the CO_2 in the formation and prevent migration back to the surface (Figure 1). When CO_2 is injected into a saline formation, it will initially be stored by stratigraphic or structural trapping, whereby the separate supercritical CO_2 phase will occupy pore space that was previously occupied by brine that was displaced during injection (Benson

and Cole, 2008). With time (decades to centuries), some or all of the injected CO_2 will dissolve into the brine to produce a homogeneous, CO_2-saturated brine, a storage process referred to as solubility trapping. Solubility trapping requires about 50% less volume compared to stratigraphic or structural trapping, and also significantly increases storage security (Steele-MacInnis et al., 2012). Eventually (100s to 1,000s of years), some of the CO_2-saturated brine will interact with minerals in the formation and precipitate carbonate minerals (calcite), resulting in mineral trapping – this is the most secure form of storage.

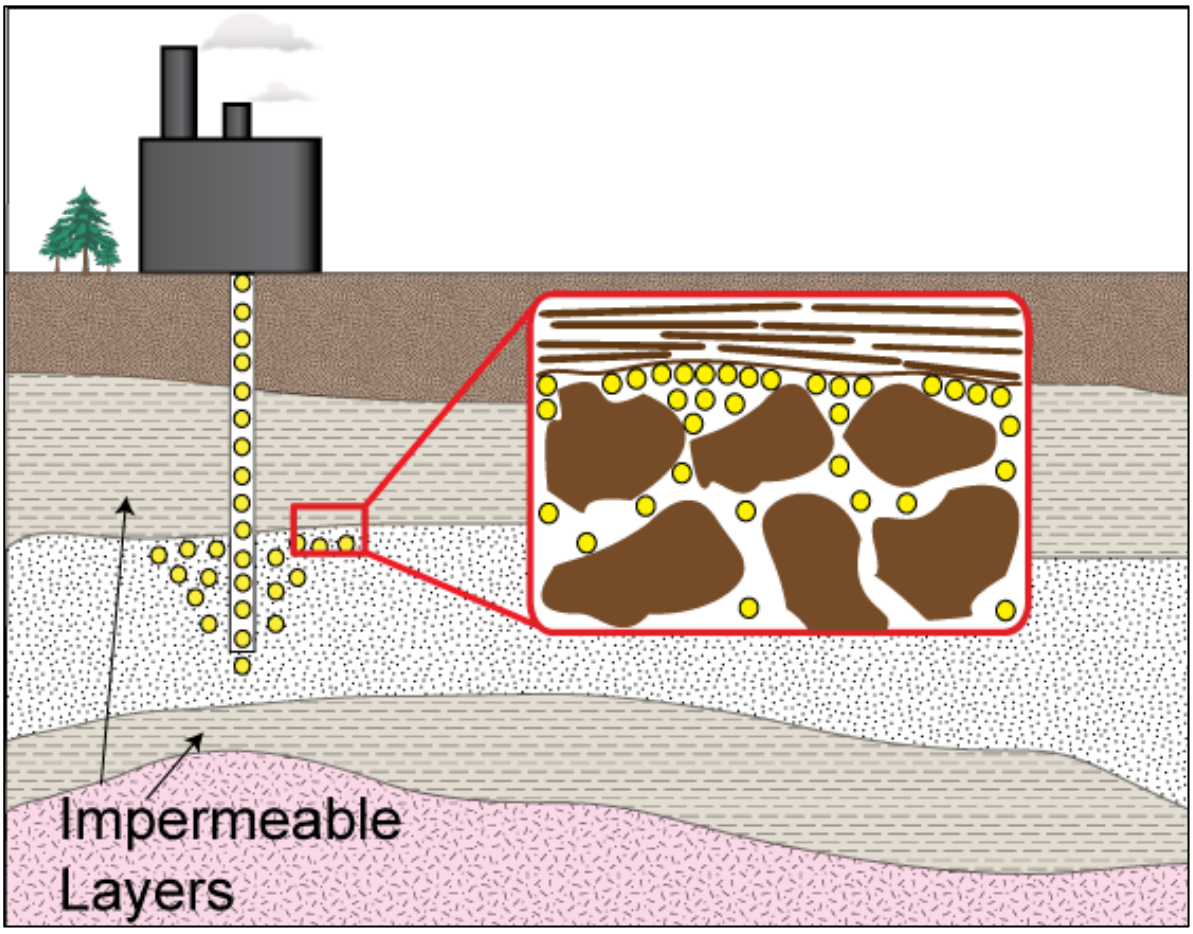

Figure 1: Schematic representation depicting the injection of CO_2 emissions from a fossil fuel power plant into a saline formation beneath an impermeable shale cap rock. The CO_2 (yellow circles) is buoyant relative to the saline brine in the pores and rises to the top of the formation where it may interact with the clay-rich shale cap rock.

During the initial stages of the CCUS process when structural and stratigraphic trapping dominate, the more buoyant supercritical CO_2 phase will tend to rise and accumulate at the top of the permeable formation, beneath the impermeable confining layer (Figure 1). In many sedimentary basins containing deep, saline formations that might be accessed for CCUS, an effective and common cap rock is shale, which is composed mainly of various types of clay minerals and quartz (Benson and Cole, 2008; Shaw and Weaver, 1965). The accumulated CO_2 will thus interact with the minerals in the confining unit during the stage in which structural and stratigraphic trapping dominate, and this interaction may affect the quality of the seal and the long-term storage security.

1.2 *Study Objectives*

In this study, we investigated potential effects on the long-term storage security of a saline formation overlain by shale by examining the interaction of CO_2 with the clay mineral montmorillonite (Figure 2). Montmorillonite is a member of the smectite group of clays, which are characterized by their ability to incorporate various elements or species into their structure and thus change their volumes, classifying them as "swelling clays" (Klein, 2001). Cap rocks that contain significant amounts of swelling clays have the possibility to modify the cap rock permeability upon exposure to CO_2 (Suekane et al., 2008). Such changes may enhance or degrade the quality of the seal and long-term storage security. By improving our understanding of how CO_2 interacts with montmorillonite at CCUS temperature and pressure conditions, we will be able to better choose appropriate geologic environments for sequestration and predict with a higher degree of confidence the long-term behavior of the formation. Using Attenuated Total Reflectance-Fourier Transform Infrared Spectroscopy (ATR-FTIR), Na-rich montmorillonite was systematically exposed to pure CO_2 under conditions of increasing and

decreasing pressure to identify crystallographic locations (AlAlOH, AlMgOH and interlayer) within the montmorillonite structure where CO_2 might interact with this mineral.

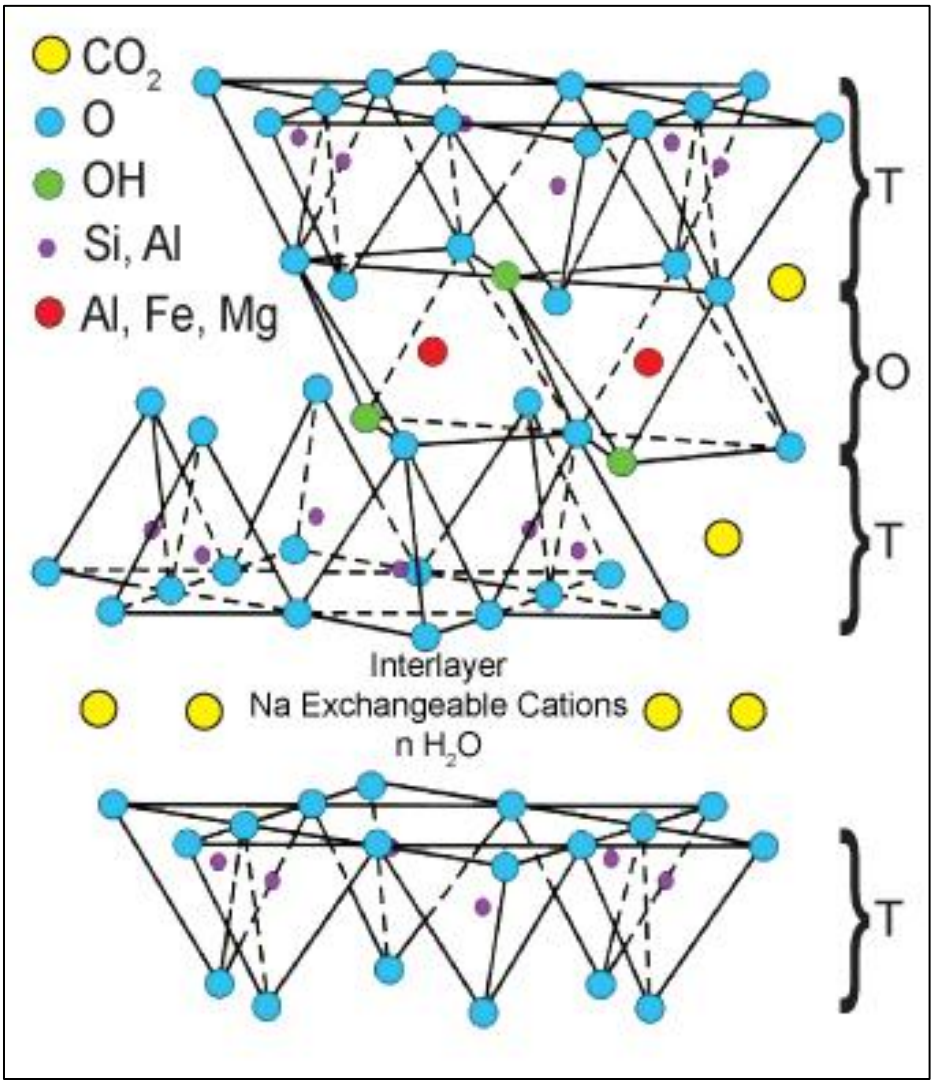

Figure 2: The crystallographic structure of montmorillonite viewed along [100]. The CO_2 (yellow circles) could interact with montmorillonite at several locations within the structure, including the interlayer space and along the edge of the TOT sheets. Modified from Grim (1962).

2. BACKGROUND

2.1 *Smectite Background*

The smectites mineral group, which includes montmorillonite, is a group of clays with an Si:O ratio of 2:1, which means they have a tetrahedral-octahedral-tetrahedral (TOT) structure, as shown in Figure 2 (Murray, 2007). Smectites are referred to as "swelling clays" because of the tendency for fluids to be taken up between the layers in the mineral structure, causing the clay to expand (Yamada et al., 1994). The expansion of the interlayer spacing, the space between each TOT sheet, depends upon the amount of H_2O between each sheet (in the interlayer), which is directly related to the hydration state of the clay. The dehydrated interlayer space is ~10 Å, spacing for a single layer of hydration (1w) is ~12.4 Å and a double layer of hydration (2w) spacing is ~15.2 Å (Yamada et al., 1994). Nonstructural H_2O in the interlayer space can be replaced by other molecules, including CO_2. A primary CCUS storage issue concerns how much CO_2 might be incorporated into montmorillonite in the caprock during and following injection, and how long CO_2 would remain sequestered in the smectite interlayers if the integrity of the cap rock seal is compromised. This could lead to a pressure drop in the reservoir, migration of CO_2 into the overlying formations, and possibly the eventual escape of CO_2 into the atmosphere. In order to better understand potential interactions between CO_2 and caprocks at CCUS conditions, we examined CO_2 adsorption and desorption in a Na-rich montmorillonite variety of smectite.

2.2 *Montmorillonite Background*

Montmorillonite [$(Na,Ca)_{0.3}(Al,Mg)_2Si_4O_{10}(OH)_2 \cdot n(H_2O)$] is a common type of smectite typically formed as a weathering product from volcanic ash (Klein, 2001; Van Olphen and Fripiat, 1979). It is also found in clay rich shales, which serve as cap rocks above many

formations suitable for carbon sequestration (De Caritat et al., 1997; Murray, 2007). The crystal structure of montmorillonite is TOT, and the two tetrahedral sheets are composed mainly of Si and O. Al can replace the Si in the center of tetrahedra if the sample is enriched in Al. An octahedral sheet composed of OH, Mg, Al, and sometimes Fe, occurs between the tetrahedral sheets (Grim, 1962; Madejova and Komadel, 2005). The TOT sheet has an overall negative charge which can be satisfied by interlayer cations, such as Na, Ca, or Mg. The interlayer space is also typically occupied by H_2O (nonstructural). The montmorillonite used in this study for the ATR-FTIR analyses was prepared and analyzed previously by Rother et al. (2012) for excess sorption and neutron diffraction studies.

2.3 *Background Montmorillonite Studies*

Infrared spectroscopy is an ideal method to characterize clays and to examine the hydration state of smectites and how water affects the mineral structure. The infrared spectrum of phyllosilicates was first characterized by Farmer (1974), who summarized the fundamental bending and stretching vibrations due to structural and nonstructural OH. He identified montmorillonite OH-stretching vibrations around 3630 cm^{-1} produced by structural H_2O in the clay. Bishop et al. (1994) further investigated the role of H_2O in montmorillonite by identifying structurally bound H_2O as well as surface-bonded H_2O molecules that will be removed during dehydration. Later, Bishop et al. (2001) extended these initial studies by examining interactions between H_2O and different interlayer cations in montmorillonite. Bishop found that as the montmorillonites were dehydrated, there was a significant change in the OH band intensities near 3450 cm^{-1} and 3350 cm^{-1}. However, bands that are associated with water bound to cations near 3620 cm^{-1} and 3550 cm^{-1} were not affected by the change in hydration state. This indicates that nonstructural or interlayer H_2O being removed from the sample can be observed by the absence

or reduction in intensity of peaks near 3450 cm^{-1} and 3350 cm^{-1}. Schaef et al. (2012) determined that anhydrous supercritical CO_2 exposure to 1w Ca montmorillonite would not dehydrate the sample of interlayer water, but in fact slightly expand the interlayer space. However, when anhydrous supercritical CO_2 was exposed to 2w Ca montmorillonite, the interlayer space was dehydrated causing the sample volume to shrink. Schaef et al. (2012) concluded that the interactions between CO_2 and Ca montmorillonite would depend largely on the initial hydration state of the clay.

Infrared spectroscopy and x-ray diffraction (XRD) have been applied to examine CO_2 interactions within the interlayer spacing of montmorillonite. Fripiat et al. (1974) confirmed that CO_2 does in fact enter the interlayer spacing of the smectite at low temperatures using x-ray diffraction and infrared adsorption at low temperatures. This result was later confirmed by Rother et al. (2012) based on neutron diffraction analyses and by Loring et al. (2012) using XRD. Giesting et al. (2012) further showed that Na montmorillonite swells in the presence of CO_2 with the optimum range of expansion of the interlayer (d(001)) between 10.0 and 11.5 Å with little expansion below and no expansion above these values. Busch et al. (2008) examined the CO_2 storage potential of shales and several smectites, including montmorillonite, as a possible reservoir, based on the incorporation of CO_2 into the interlayer space. Their results show that CO_2 diffusion through the formation after injection was slowed by the low permeability and expansive properties of the smectites. They concluded that the seal quality would be enhanced as a result of interaction of CO_2 with the overlying shale. Cygan et al. (2010) examined the molecular interactions associated with CO_2 intercalation into the montmorillonite based on molecular dynamics simulations. Recently, Cygan et al. (2012) modified the molecular dynamics simulation to include H_2O in the interlayer and considered diffusion of CO_2 and H_2O in the

interlayer. De Pablo et al. (2007) ran Monte Carlo simulations to predict what the hydration state of montmorillonite would be at typical sequestration depths. Their findings showed that the clay would maintain a 1w layer of hydration at CCUS temperature and pressure conditions. Botan et al. (2010) ran Monte Carlo simulations on Na-montmorillonites using a mixture of H_2O-CO_2 fluids. Their findings agree with results from Busch et al. (2008), showing some residual CO_2 remains within the montmorillonite structure after pressure is decreased.

Other studies have examined the relationship between interlayer water and the location of the interlayer cations. When water is present in the interlayer, electrostatic interactions draw the Na cation out of the ditrigonal cavities located on the edges of the TOT structure and into the interlayer spacing (Sposito et al., 1983). The interactions of montmorillonite with various organic compounds have also been characterized (Gu et al., 2011; Lee and Tiwari, 2012; Stevens and Anderson, 1996; Tzavalas and Gregoriou, 2009). Understanding how interlayer water modifies the montmorillonite structure and other physical and chemical properties of montmorillonite is necessary in order to better understand how the introduction of CO_2 into a saline formation overlain by shale cap rock might affect storage security.

3. EXPERIMENTAL SETUP

The interaction between CO_2 and Na-rich montmorillonite was studied using an Attenuated Total Reflectance-Fourier Transform Infrared Spectroscopy (ATR-FTIR). The design of the ATR-FTIR system allowed us to examine Na-montmorillonite before, during, and after exposure to CO_2, without having to remove the sample from the instrument. By systematically analyzing the clay at various pressures and at constant temperature, an isotherm for adsorption and desorption of CO_2 into and out of the montmorillonite crystal structure was obtained. The desorption isotherm was obtained by decreasing the pressure stepwise, and at each pressure collecting spectra at various times to determine if CO_2 that had been adsorbed during the increasing pressure cycle was desorbed during pressure decrease. This information is critical to understanding long-term storage security in the event of a breach in the seal after injection of CO_2 is complete.

3.1 *ATR-FTIR Setup*

The FTIR setup utilized two custom designed tunnel ATR (attenuated total reflectance) stainless steel cells from SpectraTech that were connected in tandem via 0.16 cm stainless steel tubing so that each cell experienced the same CO_2 pressure (Figure 3). A cylindrical zinc selenide (ZnSe) ATR crystal was placed inside of each cell. The ATR crystal is 2.8 cm long and 0.6 cm thick, the incidence angle was 45°, and the number of reflections within the crystal was 11. One cell contained a ZnSe ATR crystal with no sample present and the other cell contained a ZnSe ATR crystal coated with sample. Teflon O-rings were used to make a high-pressure seal between the stainless steel chamber and ATR crystal. The cells were placed on a manual

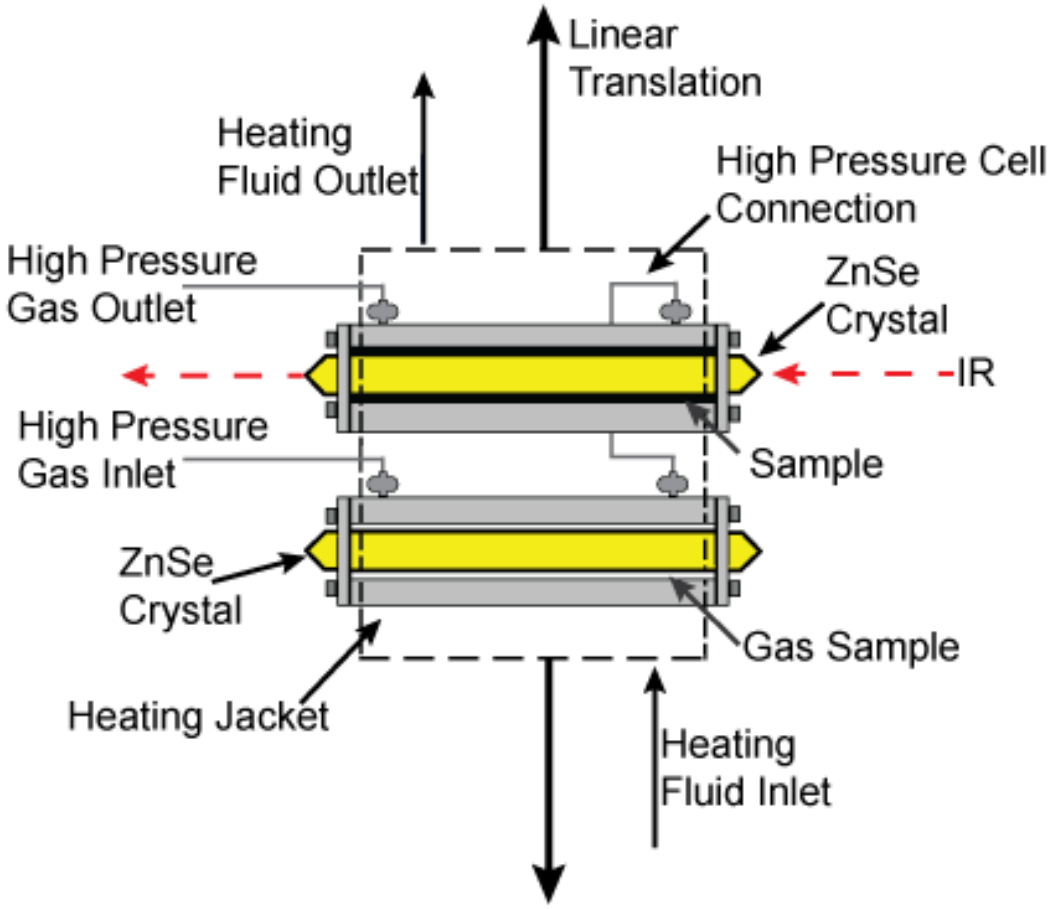

Figure 3: Schematic diagram of the ATR-FTIR cell setup. The ZnSe crystal in the top chamber was painted with a methanol + clay slurry and then the methanol was allowed to evaporate before the crystal was introduced into the cell. The second crystal (bottom chamber) was free of any contaminants and exposed to the same gas pressure as the crystal in the top chamber that was coated with sample.

translator inside the FTIR spectrometer such that they could be moved to allow infrared light to probe either the blank ATR crystal or the ATR crystal coated with the sample. Minimum penetration depth of the infrared beam into the sample is estimated to be ~1 μm. This ensures that both the bulk and surface of the sample are interrogated. The cells were enclosed in a thermal jacket that allowed a recirculating bath fluid to flow through the external jacket to either heat or cool the cells.

3.2 *Montmorillonite Sample*

Van Olphen and Fripiat (1979) characterized the sample of low-iron montmorillonite (STX-1) with a published structural formula of $(Ca_{0.27}Na_{0.04}K_{0.01})(Al_{2.41}Fe^{3+}_{0.09}Mn_{t}{}_{r}Mg_{0.71}Ti_{0.01})_2Si_8O_{20}(OH)_4$ that was procured from the Clay Mineral Repository for this study. To remove traces of calcite from the sample, it was first reacted with 1 M sodium acetate buffer at pH 5 for 2 weeks. The acetate was then removed by dialyzing the clay in deionized water until the wash conductivity was 18 MΩ cm. The sedimentation method was used to separate the <2 μm clay fraction. Then, the <2 μm clay fraction suspensions were flocculated by the addition of NaCl (5M). The clay was kept in the NaCl solution for seven days to allow complete exchange with the solution to produce a Na-montmorillonite. Lastly, the excess salt was removed by dialyzing the suspension in deionized water, followed by freeze-drying as described by Rother et al. (2012).

3.3 *FTIR Sample Preparation*

To prepare the sample for analysis, the Na-rich montmorillonite was immersed in methanol to form a slurry. A small amount of the slurry (~10 mg) was then painted onto the ZnSe ATR crystal to form a thin layer. After evaporating the methanol, the montmorillonite-coated crystal was placed inside the cell, being careful to not tilt or bump the crystal and dislodge some of the sample, and the sample port was sealed. The sample chamber was flushed with ultra-high purity nitrogen for at least 24 hours before analysis. Complete desorption (evaporation) of methanol used during sample preparation was verified by the absence of IR absorption bands at 2960, 2844, 1345, and 1033 cm^{-1} corresponding to methanol (Shimanouchi, 1977). To examine the effect of pressure on CO_2 interaction with montmorillonite, the ATR cell assembly was connected to a gas handling system consisting of a syringe pump (ISCO model

260D), a port for gas introduction, and a pressure transducer (OmegaDyne Inc PX01K1-5KGV). The total volume of the system was estimated to be 1 ml. All ATR-FTIR data were collected with a single-beam FTIR spectrometer (Thermo Electron Nexus 4700 FTIR ESP) equipped with a wide-band MCT detector. Unless otherwise noted, 200 scans were collected with an instrument resolution of 2 cm^{-1} over the spectral range extending from 4000 to 600 cm^{-1}. The sample was equilibrated with either carbon dioxide or nitrogen before analyses. Carbon dioxide (99.998% supercritical grade) and ultra-high purity nitrogen (UHP) were used as supplied from Butler gas. The Na-rich montmorillonite material was investigated at 35 and 50 $^{\circ}C$, and CO_2 pressure 0-1000 psi. After changing the pressure, equilibrium was achieved within 15 minutes as evidenced by spectra that remained unchanged after this amount of time. The blank and sample ATR cells were thermally equilibrated by circulating a 50:50 ethylene gycol:water mixture (NESLAB RTE 7) through the temperature jacket.

3.4 *Data Processing*

Two transmission spectra were recorded at each point: one from the cell containing both CO_2 and sample (Figure 4A, black spectrum) and one from the cell containing CO_2 (Figure 4A, grey spectrum). The raw transmittance data was processed by applying a negative log conversion to translate data to absorbance according to the Beers Law (Figure 4B)(Günzler and Heise, 2002). The sample chamber holds both a blank and a sample crystal at the same CO_2 pressure (Figure 3). Thus, in addition to bands associated with CO_2 adsorbed onto the clay sample, bands associated with gaseous CO_2 are also recorded for the crystal coated with the montmorillonite sample. The final absorption spectrum of CO_2 was obtained by subtracting the blank spectrum from the total absorbance spectrum in Figure 4B to obtain the final sample spectrum, shown in Figure 4C.

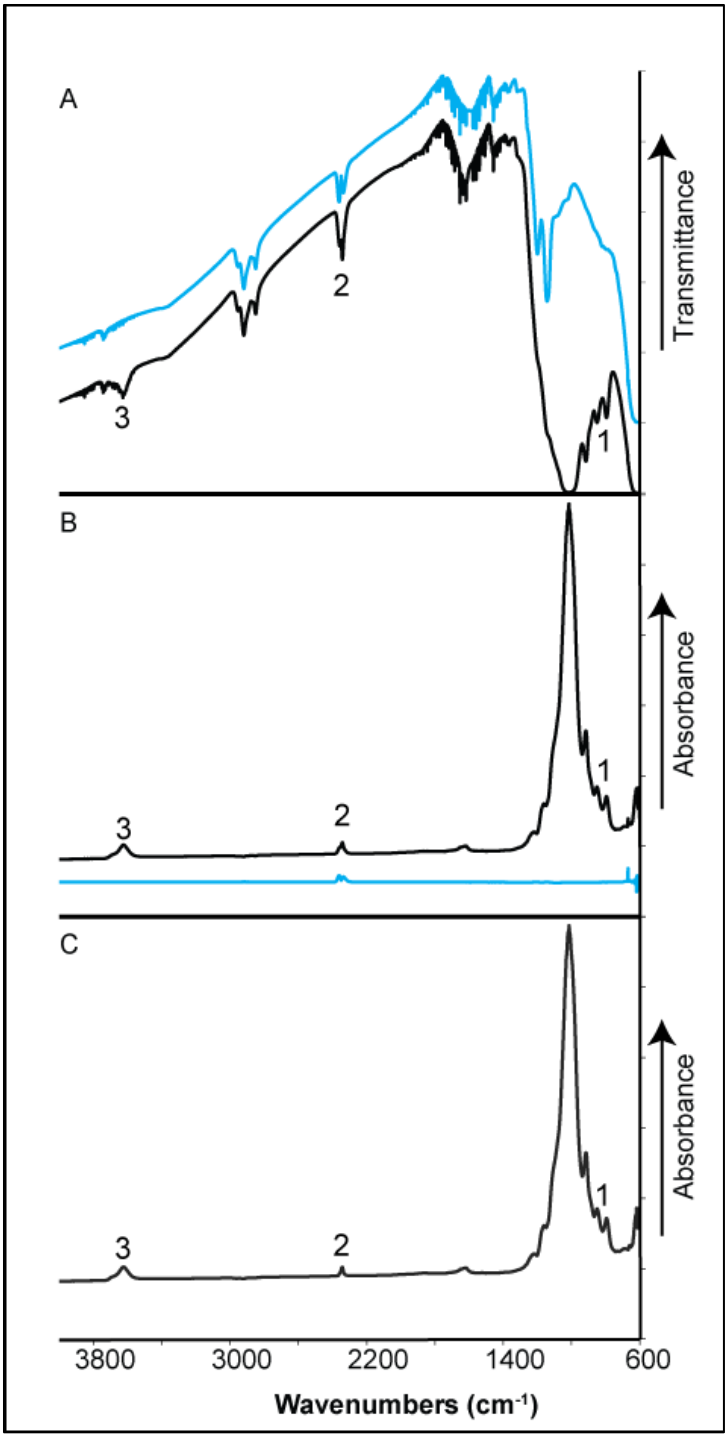

Figure 4: Representative FTIR spectra obtained in this study. The labeled peaks correspond to: 1, AlMgOH (841 cm^{-1}); 2, v_3 CO_2 (2343 cm^{-1}); 3, Al enrichment in octahedral positions (3620 cm^{-1}). Figure 4A shows the raw data in transmittance as a function of wavenumber (cm^{-1}). Figure 4B shows the same data transformed to absorbance according to Beers Law. Figure 4C shows the final spectrum after subtraction of the CO_2 in the blank chamber from that in the chamber with the sample to give the spectrum of CO_2 remaining in the sample.

Peak position (PP) changes and peak area (PA) changes were determined according to equations 1 and 2, shown below.

$$PP = PP_{P,T} - PP_{R} \quad \textbf{(1)} \qquad PA = \left(\frac{PA_{P,T} - PA_{R}}{PA_{R}} \right) * 100 \quad \textbf{(2)}$$

The variables are defined as follows: $PP_{P,T}$ refers to peak position at conditions of interest, PP_R refers to the reference peak position, $PA_{P,T}$ refers to peak area at conditions of interest, and PA_R refers to the reference peak area. Equation 1 refers to the change in peak position from the reference peak position. A shift in the peak position greater than 2 cm^{-1} (analytical precision) would indicate a chemical interaction. Equation 2 refers to the percent change in the peak area of interest from the peak area reference. A change in the peak area would indicate more or less of that bond vibration being present within the sample.

4. RESULTS AND DISCUSSION

The montmorillonite sample was initially introduced into the FTIR chamber and placed under vacuum to analyze the spectrum prior to exposure to pressure or CO_2. The next test was to determine if the montmorillonite structure would be modified (as evidenced by variations in the FTIR spectrum) by changing temperature and pressure over the range of P-T conditions planned for the CO_2 experiments. To accomplish this, the montmorillonite sample was analyzed at various pressures using N_2 gas as the pressure medium. Then, the nitrogen gas was purged from the system and CO_2 gas was pumped into the sample and blank chambers. The CO_2 pressure was increased and held at pressure for approximately 4 hours, with spectra recorded after 15 minutes, after 2 hours 20 minutes and after 4 hours to determine if the spectral characteristics change as a result of the duration of exposure to CO_2. Next an increase in CO_2 pressure from 0-1000 psi was tested to examine any interactions. The sample, previously analyzed at 35 °C, was then analyzed at 50°C to examine temperature effects. Next, the hydration state of the clay was determined and the hydrated montmorillonite was dehydrated and analyzed in the presence of nitrogen to determine if the spectral characteristics varied as a function of hydration state. Then, the same experiment was conducted in the presence of CO_2. The hydrated sample was dried to remove nonstructural H_2O residing in the interlayer space of the clay and the dehydrated sample was exposed to CO_2. The spectrum of the hydrated sample was compared to that of the dehydrated sample.

4.1 *Background Spectrum*

Before CO_2 was introduced into the sample chamber, a background spectrum was collected of the Na-rich montmorillonite starting material. The peaks observed include: (1) cristobalite at 791

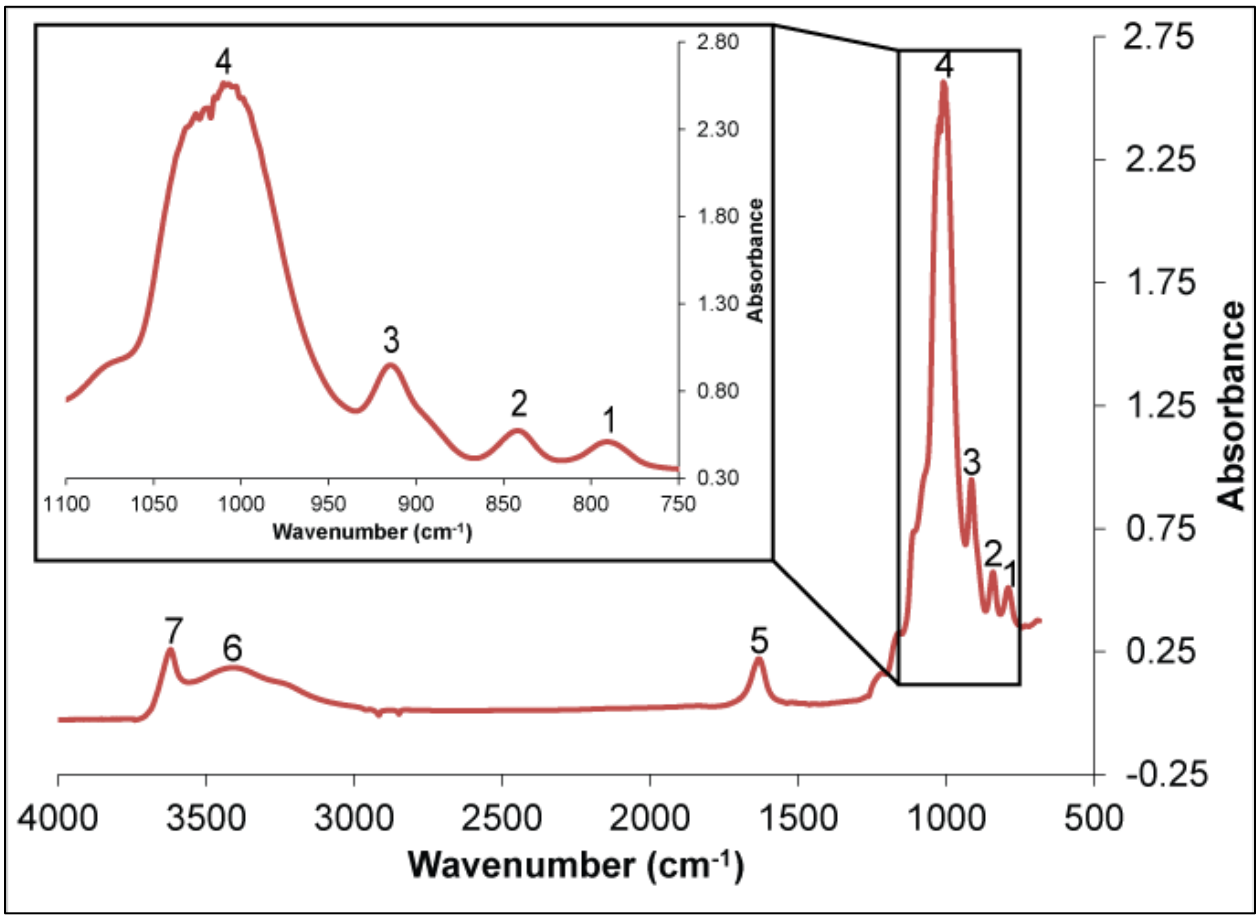

Figure 5: FTIR spectrum of montmorillonite without CO_2 present in the cell. The labeled peaks correspond to: 1, cristobalite (791cm^{-1}); 2, AlMgOH (841 cm^{-1}); 3, AlAlOH (914 cm^{-1}); 4, Si stretching mode (1030 cm^{-1}); 5, OH bending mode (1630 cm^{-1}); 6, OH asymmetric and symmetric stretch (~3400 cm^{-1}); 7, aluminum enrichment in octahedral positions (~3620 cm^{-1}).

cm^{-1}, (2) AlMgOH at 841 cm^{-1}, (3) AlAlOH at 914 cm^{-1}, (4) Si stretching mode at 1030 cm^{-1}, (5) OH bending mode at 1630 cm^{-1}, (6) OH asymmetric and symmetric stretch at ~3400 cm^{-1} and (7) aluminum-enriched octahedral positions at ~3620 cm^{-1} (Figure 5). All peaks were identified according to data from Madejova and Komadel (2005). The AlAlOH band at 914 cm^{-1} and the AlMgOH band at 841cm^{-1} were used to monitor changes in the Na-rich montmorillonite crystal structure during exposure to CO_2. Residual cristobalite occurs in the sample and was identified based on a peak at 791 cm^{-1} (Madejova and Komadel, 2005; Rother et al., 2012). Also, expansion of the water peak at ~3621 cm^{-1} due to aluminum enrichment in the octahedral

position of the clay was recognized. This expansion in the OH region has been well documented in both Al- and Fe-rich montmorillonites, (Bishop et al., 2001; Madejova and Komadel, 2005). The initial scan of our sample confirmed that the montmorillonite sample was hydrated due to exposure to air before loading the sample into the infrared spectrometer, evidenced by a peak at ~3400 cm^{-1} associated with nonstructural H_2O. The location, identity, and spectral characteristics of all montmorillonite peaks were characterized prior to CO_2 exposure. While Giesting et al. (2012) hypothesized a possible carbonate forming in the interlayers of a Na montmorillonite, no evidence for this was found in this study, which agrees with the findings from Loring et al. (2012).

4.2 *Pressure Test*

The montmorillonite was characterized in an N_2 environment and in a CO_2 environment. The assumption is that analysis in the nitrogen environment would provide information on pressure effects without any chemical interaction between the gas and the montmorillonite for later comparison with the CO_2 experiments. The hydrated sample was analyzed at ~250 and ~1280 psi, first with N_2 as the pressure medium and then with CO_2. When compared to the spectrum of the montmorillonite before exposure to any gas (i.e., at ambient pressure), all of the characteristic montmorillonite peaks were present and unchanged during exposure to N_2, indicating that N_2 does not interact with the montmorillonite structure and that pressure alone does not affect peak position or area, at least over the range of pressures of this study (Figure 6). When the sample was analyzed in the presence of CO_2, the montmorillonite peak positions were unchanged, however, the area of the O-H stretching band (~3400 cm^{-1}) associated with the

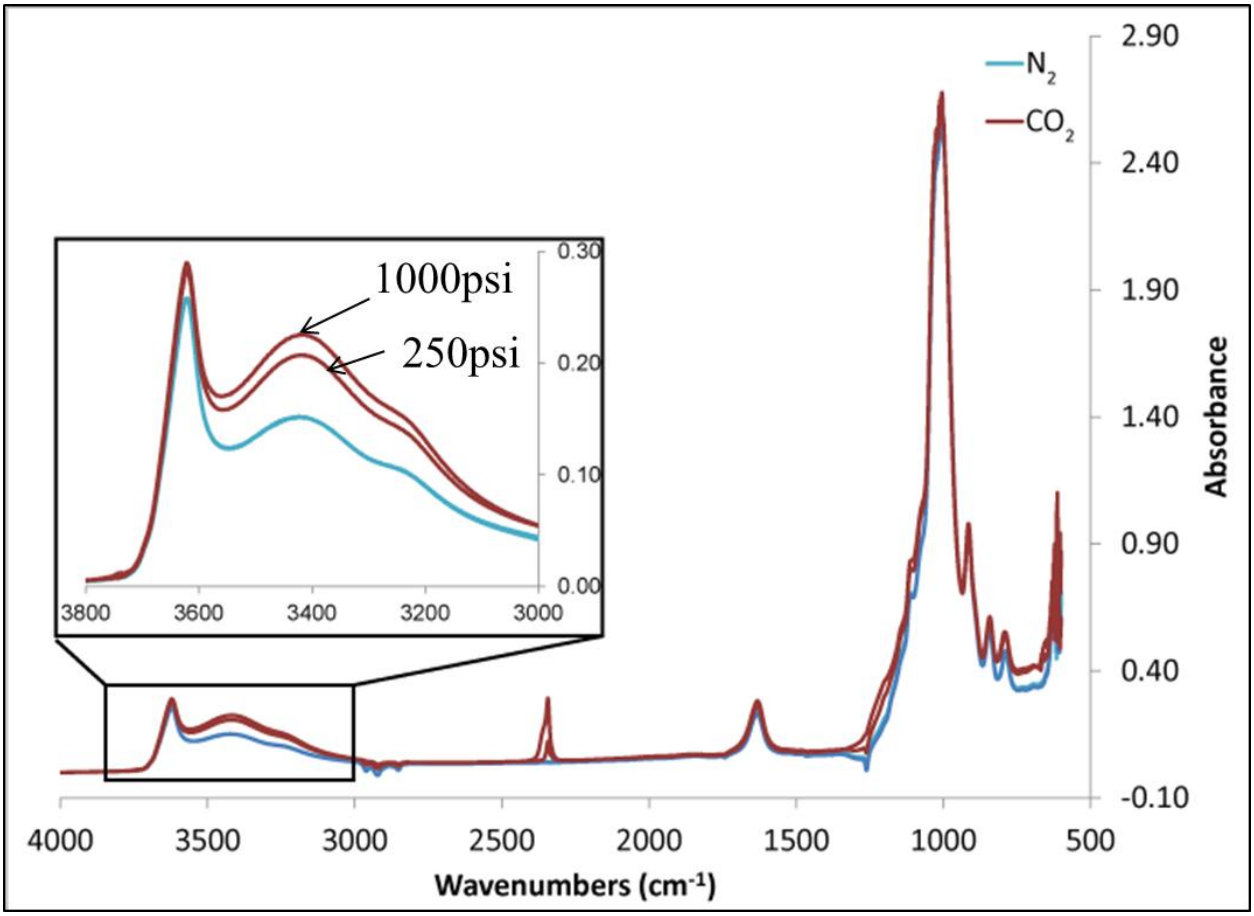

Figure 6: Comparison of the bands from the hydrated montmorillonite sample when exposed to N_2 and CO_2 atmosphere. The blue spectrum represents the sample in a nitrogen atmosphere at 266 and 1260 psi while the red spectrum represents the sample in a CO_2 atmosphere at 251 and 1275 psi.

interlayer water increased as shown in Figure 6. As CO_2 enters into the interlayer space, it fills space not occupied by water and thus further restricts the remaining interlayer water to a smaller volume. With the addition of CO_2, the physical adsorption of CO_2 onto the hydrated montmorillonite was evidenced by the CO_2 v_3 antisymmetric stretch band at 2343 cm^{-1} and the CO_2 v_2 bending mode at 659 cm^{-1} (Figure 7) (Flichy et al., 2001; Goodman, 2009).

4.3 *Equilibration Time*

After the spectrum of the montmorillonite was characterized in the absence of CO_2, experiments were conducted to examine the effect of CO_2 on the crystal structure and the mechanisms of CO_2 interaction with montmorillonite. The first step was to determine the amount

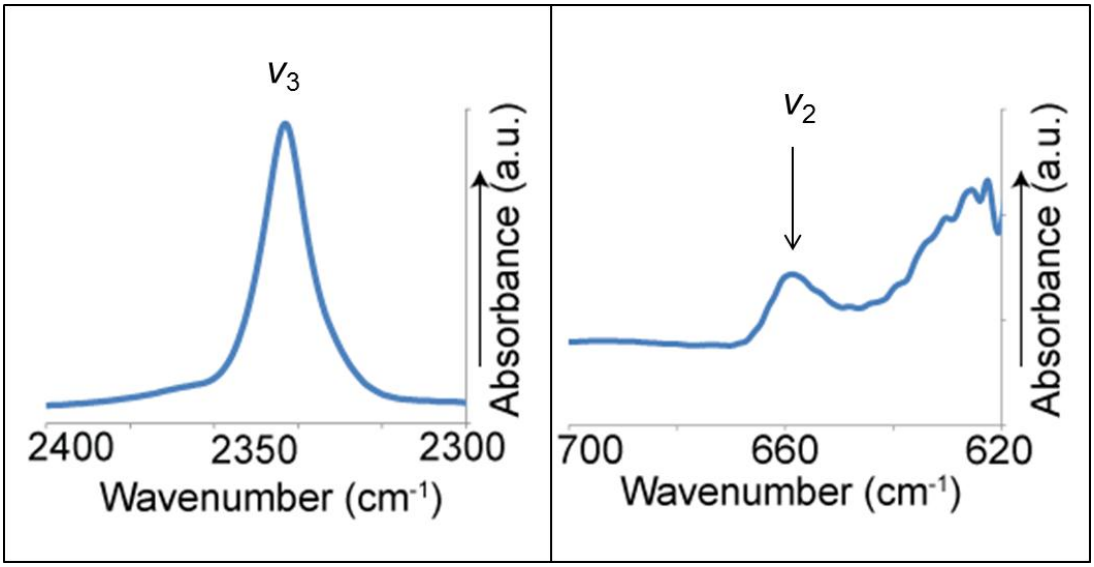

Figure 7: Shown left is CO_2 v_3 antisymmetric stretch band at 2343 cm^{-1} and on the right is CO_2 v_2 bending mode at 659 cm^{-1} in the hydrated montmorillonite sample.

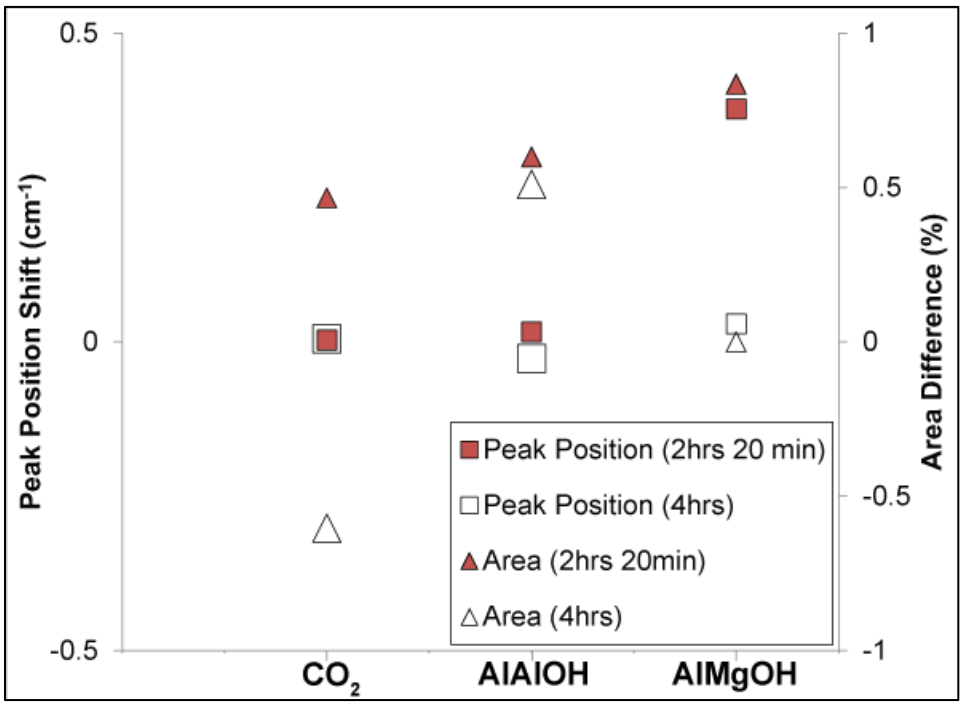

Figure 8: The effect of time on the peak position and peak area for the v_3 CO_2, AlAlOH, and AlMgOH bands in the montmorillonite sample at 78 psi CO_2 pressure. No systematic or significant changes in the spectrum were observed as a function of time at pressure. For the v_3 CO_2, AlAlOH, and AlMgOH bands, the area differences were less than 1% while the peak position shifts were within the analytical precision of the measurement (±2 cm^{-1}).

of time required for the system to reach equilibrium after the pressure is changed. To accomplish this, the sample was exposed to 64 psi CO_2 pressure and analyzed after 15 minutes, 2 hours 20 minutes, and 4 hours. No significant difference in peak position or peak area for the v_3 CO_2, AlAlOH, or AlMgOH peaks was observed (Figure 8). In order to systematically examine interactions between CO_2 and the montmorillonite structure, the sample was analyzed at a variety of conditions.

4.4 *Peak Position and Peak Area Changes with CO_2 Pressure*

At low CO_2 pressure (78 psi) the AlAlOH or AlMgOH peak positions and areas were unchanged compared to the measurements at ambient conditions (Figure 9). After this initial analysis, CO_2 pressure was increased stepwise in ~200 psi increments, from 78 psi to 1067 psi. At each new pressure, the difference between the peak position at that pressure and the peak position at the lowest pressure (78 psi) was determined, and peak position remained constant within the analytical precision of 2 cm^{-1} (Figure 9).

The area difference was determined for v_3 CO_2, AlAlOH, and AlMgOH as shown in Figure 10. The area of the v_3 CO_2 peak increases with increasing pressure, while the peak positions and areas for the AlAlOH and AlMgOH peaks for montmorillonite remain unchanged at all pressures. This behavior is interpreted to indicate that increasing amounts of CO_2 are entering the interlayer spacing of the clay as pressure increases, but that the CO_2 is not chemically interacting with the AlAlOH and AlMgOH sites.

4.5 *Temperature Effects*

To test the effect of temperature on CO_2 - montmorillonite interactions, the same hydrated montmorillonite was run at 35 and 50°C and ~50 psi. No significant differences

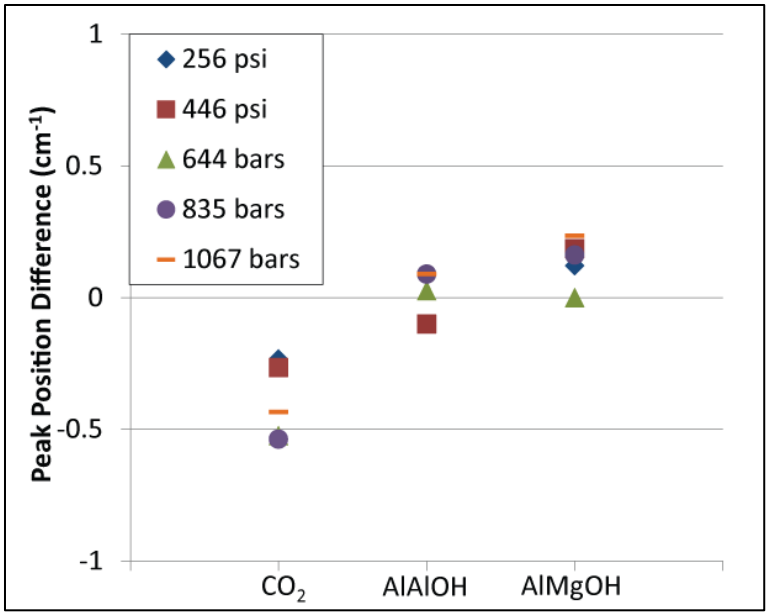

Figure 9: The effect of CO_2 pressure on positions of v_3 CO_2, AlAlOH and AlMgOH peaks. With increasing pressure no systematic or significant difference in v_3 CO_2, AlAlOH and AlMgOH peak position is observed, within the analytical precision of ~2 cm^{-1}.

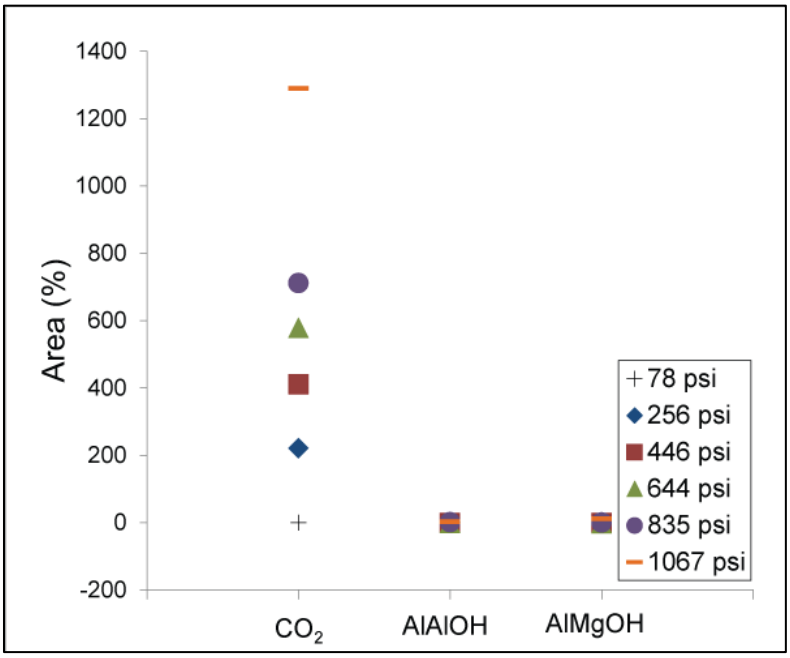

Figure 10: Comparison of increasing pressure effects versus peak area on v_3 CO_2, AlAlOH and AlMgOH. As pressure increases within the sample, the peak area of the v_3 CO_2 increases significantly. This indicates more CO_2 present in the sample. The AlAlOH and AlMgOH peak areas do not significantly change with increasing pressure.

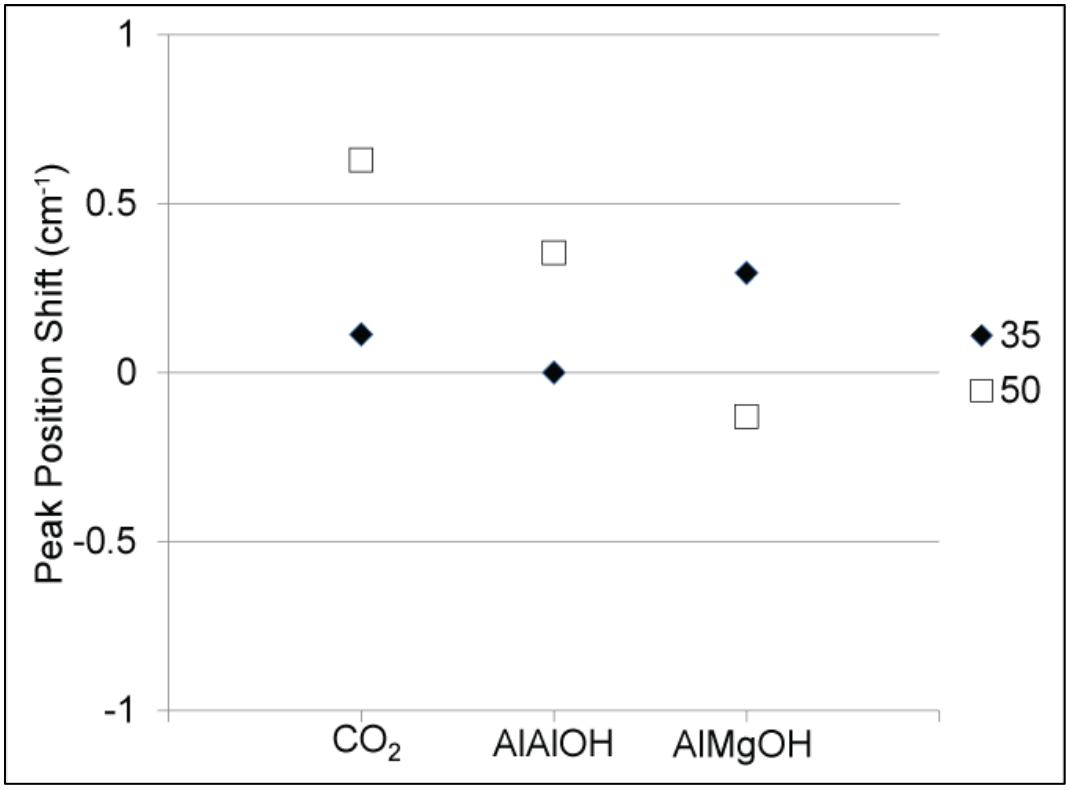

Figure 11: Effect of temperature on peak positions. No significant peak position changes were observed for the v_3 CO_2, AlAlOH, or AlMgOH peaks between 35 and 50°C (>2 cm^{-1}).

(within resolution of the instrument, ~±2 cm^{-1}) in peak positions or areas for the AlAlOH, AlMgOH and CO_2 v_3 were observed, shown in Figure 11.

4.6 *Hydration Effects*

To examine potential effects of changing the hydration state of the montmorillonite, the as received hydrated sample was dehydrated. The sample was dehydrated by raising the temperature in the cell to 100°C for approximately 1 hour in N_2 gas at ~14.7 psi. Spectra were collected before, during and after heating to monitor any changes in the OH region at ~3400 cm^{-1}. There was a decrease noted in the OH region at ~3400 cm^{-1}, corresponding to a decrease of nonstructural, or interlayer, water in the sample (Figure 12A). Sposito et al. (1983) noted a shift

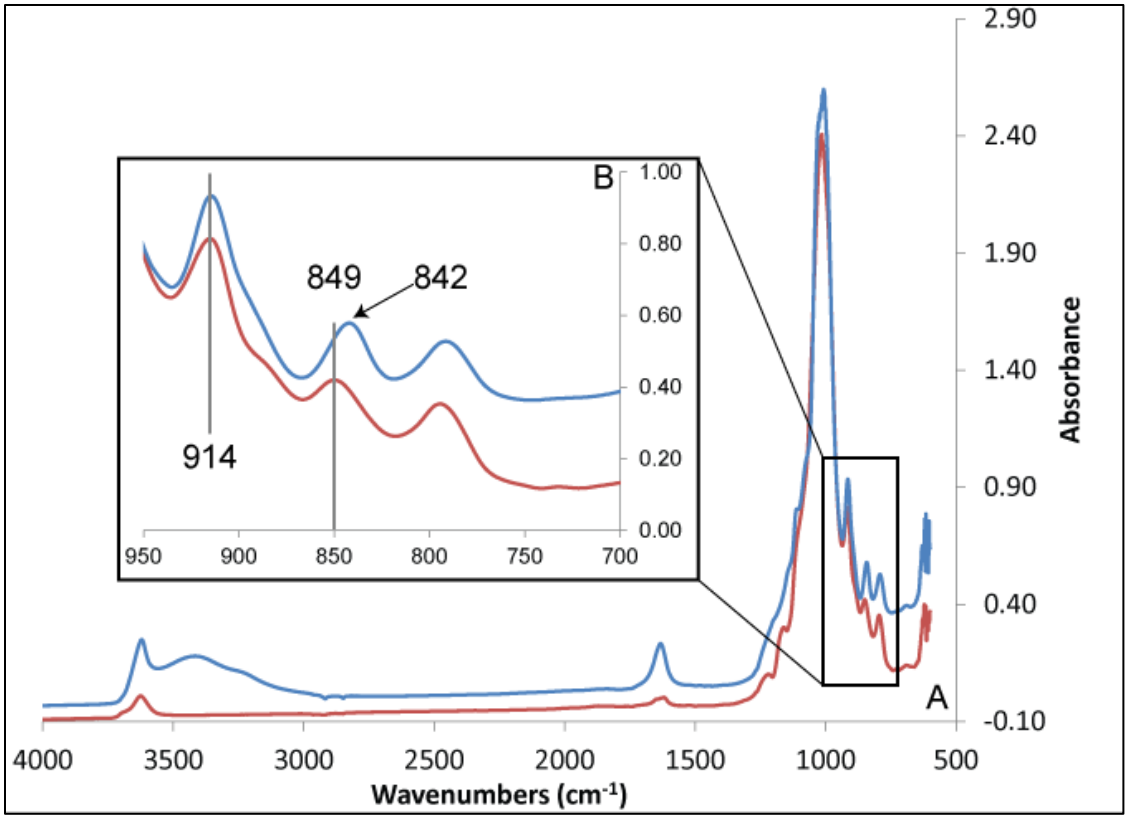

Figure 12: Comparison of spectra of hydrated and dehydrated montmorillonite with no CO_2 present. The red spectrum represents the hydrated montmorillonite sample, while the blue spectrum represents the dehydrated montmorillonite sample. Figure 12B shows that after the sample is dehydrated, the AlMgOH peak shifts from 842 to 849 cm^{-1}, which Sposito et al. (1983) showed to be characteristic of a dehydrated sample.

in the AlMgOH peak position due to a shifting of the interlayer cations as the sample is dehydrated. The same shifts in peak position were also exhibited in our data, shown in Figure 12B. These effects were characterized and compared to the hydrated sample to note any change prior to CO_2 exposure.

CO_2 at ~50 psi and 35 °C was introduced into the sample chamber and no shift in peak position was observed, indicating that no chemical interaction between the CO_2 and the dehydrated montmorillonite occurred (Figure 13). A well-defined v_2 CO_2 peak at ~659 cm^{-1} was present in the dehydrated sample at 842 psi (Figure 13C). For the hydrated sample, the v_2 peak

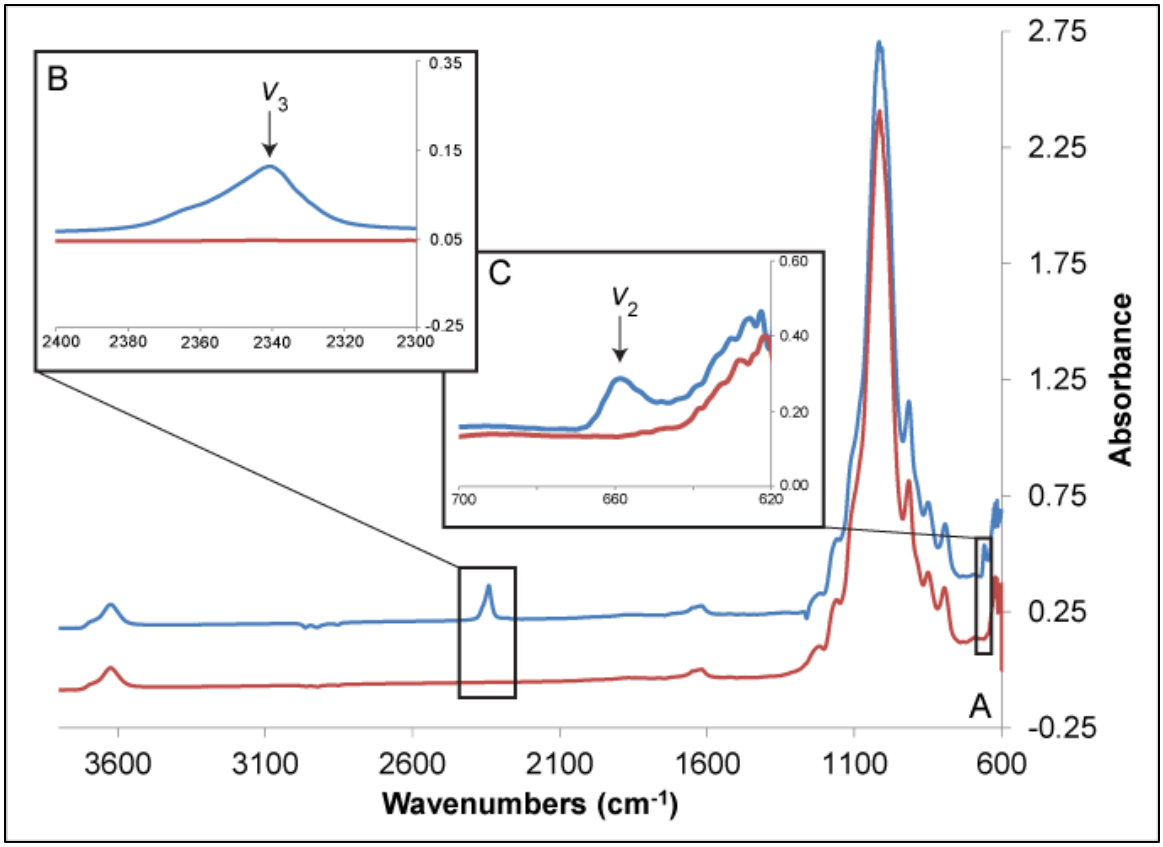

Figure 13: Comparison of the spectrum of dehydrated montmorillonite in the absence of CO_2 and in the presence of CO_2. In Figure 13A, the red spectrum represents the dehydrated sample without CO_2 present, while the blue spectrum represents the dehydrated sample at 938 psi CO_2 pressure. Figure 13B shows the v_3 CO_2 antisymmetric stretch at (2343 cm^{-1}) and Figure 13C shows a well-defined v_2 CO_2 bending mode at 659 cm^{-1} when CO_2 is present, compared to the absence of this peak in the spectrum without CO_2 present.

was very broad and not well defined at 1260 psi (Figure 14C). However, the area of the v_3 CO_2 peak in the dehydrated sample (Figure 13B) was more intense than that for the hydrated sample (Figure 14B), suggesting that the dehydrated sample can accommodate more CO_2, probably owing to a lack of nonstructural H_2O in the interlayer to interfere with and block CO_2 from this site. After completing the analyses of the dehydrated sample described above, the sample was rehydrated to 74% relative humidity and the analyses were repeated. The new experiments exhibited all the same spectral characteristics as the naturally-hydrated sample originally analyzed.

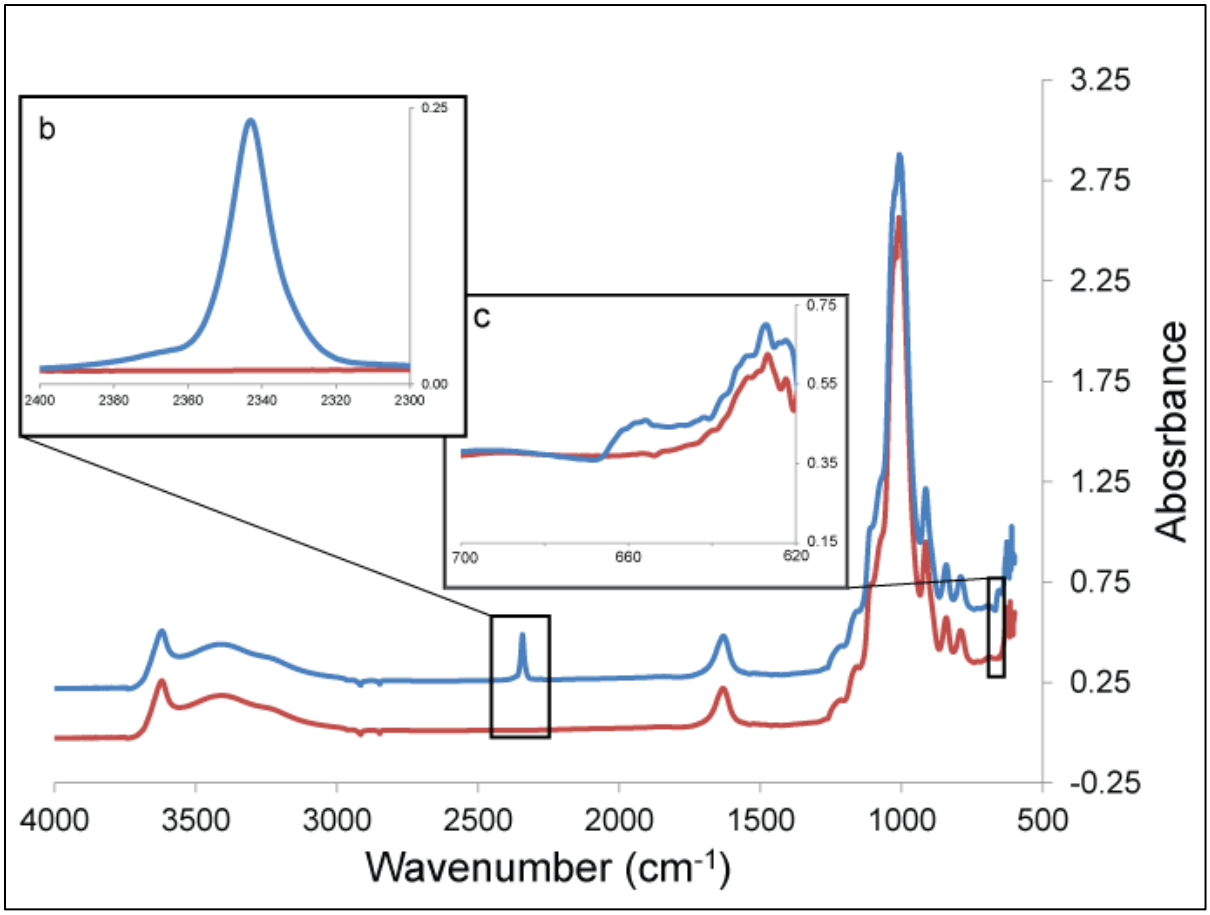

Figure 14: Comparison of the spectrum of re-hydrated montmorillonite in the absence of CO_2 and in the presence of CO_2. In Figure 14A, the red spectrum represents the re-hydrated sample without CO_2 present, while the blue spectrum represents CO_2 in the sample at 1053 psi. Figure 14B shows the region of the v_3 CO_2 antisymmetric stretch (2343 cm^{-1}) and Figure 14C shows a poorly defined v_2 CO_2 bending mode at (659 cm^{-1}) compared to the absence of peaks in the spectrum without CO_2 present.

The spectrum for the sample with CO_2 is offset from that for the sample without CO_2 on the Figure 14A due to the overlap in all regions except that for the CO_2 vibrations, the spectra are not offset in Figures 14B or 14C. When the sample is dehydrated, the v_2 and v_3 bands are still present (Figure 13). In Figure 13A the spectra are offset to show all the peaks, but Figure 13B and 13C are not offset. Chemical interaction between montmorillonite and CO_2 would be evidenced by a permanent shift in the positions of the v_2 CO_2, v_3 CO_2, AlAlOH or AlMgOH peaks. No such shifts were present in the data, therefore no chemical interactions occurred.

4.7 *Desorption Isotherms*

After the highest CO_2 pressure (~1090 psi) was reached, the pressure was decreased to ~600 psi and held at this pressure for ~24 hours to examine the CO_2 retention behavior of hydrated montmorillonite. Three spectra were collected within the first few hours after dropping the pressure, and four additional spectra were collected starting at ~18 hours after dropping the pressure. For each time step, the reference peak positions used was determined at 1090 psi CO_2 pressure was subtracted from the peak position at each time step when held at ~600 psi, and the difference is plotted in Figure 15. No significant change in peak position within the analytical precision ($\pm 2 cm^{-1}$) was observed, indicating no time-dependent retention of CO_2 within the clay structure. The peak area is thought to be proportional to the amount of CO_2 in the sample, and the peak area difference shows an increase of the CO_2 peak with time (Figure 16). At a constant pressure, the amount of CO_2 in the sample slightly increases while the AlAlOH and AlMgOH peak areas remain approximately the same. The nonstructural water peak area (~3400 cm^{-1}) in the hydrated sample decreases significantly with time (Figure 17). This indicates that CO_2 dehydrates the interlayer of excess water, i.e., CO_2 forces water out of the interlayer space and fills that space with CO_2.

4.8 *Residual CO_2*

A simulation of cap rock failure in a natural environment was conducted to observe its effects on the montmorillonite. The pressure on the sample, both hydrated and dehydrated, was initially at ~100 psi then reduced to ~14.7 psi or atmospheric conditions. When the CO_2 pressure is reduced to ~atmospheric pressure, residual CO_2 remains within the sample, as evidenced by the presence of a measureable v_3 CO_2 peak (Figure 18). This would indicate that a small, but

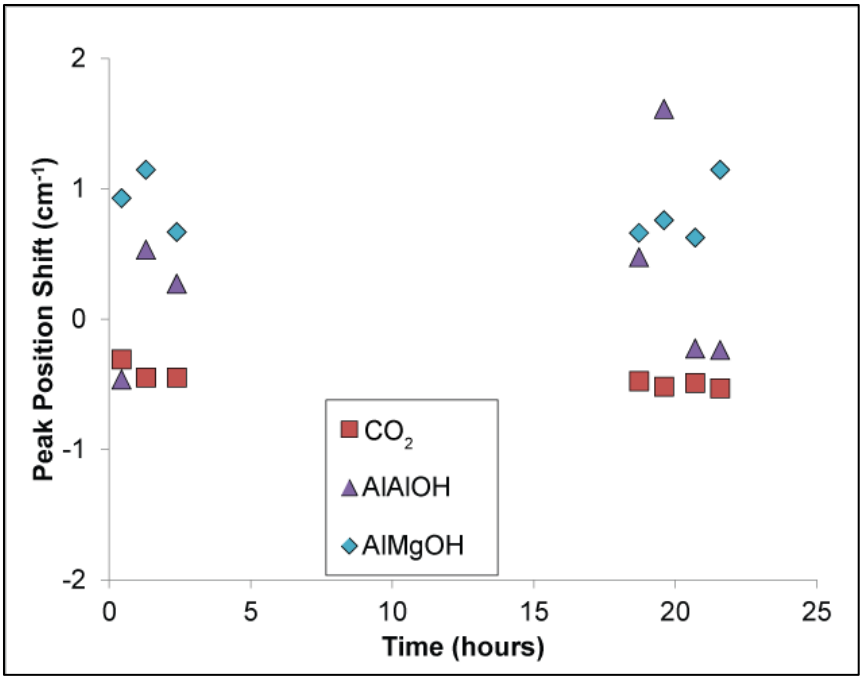

Figure 15: Peak position shift as a function of the amount of time that the sample is exposed to ~600 psi CO_2. No systematic or significant changes in the v_3 CO_2, AlAlOH, or AlMgOH peak positions are observed.

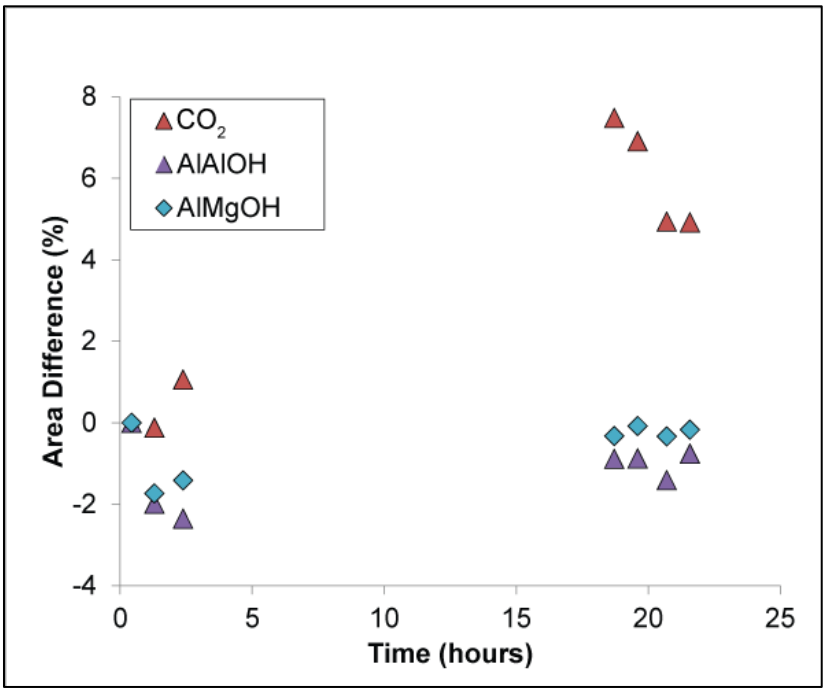

Figure 16: Peak areas as a function of the amount of time that the sample is exposed to ~600 psi CO_2. No systematic or significant changes in the AlAlOH or AlMgOH peak areas were observed. The area under the v_3 CO_2 peak does increase by ~8% indicating that more CO_2 is being incorporated into the sample with time.

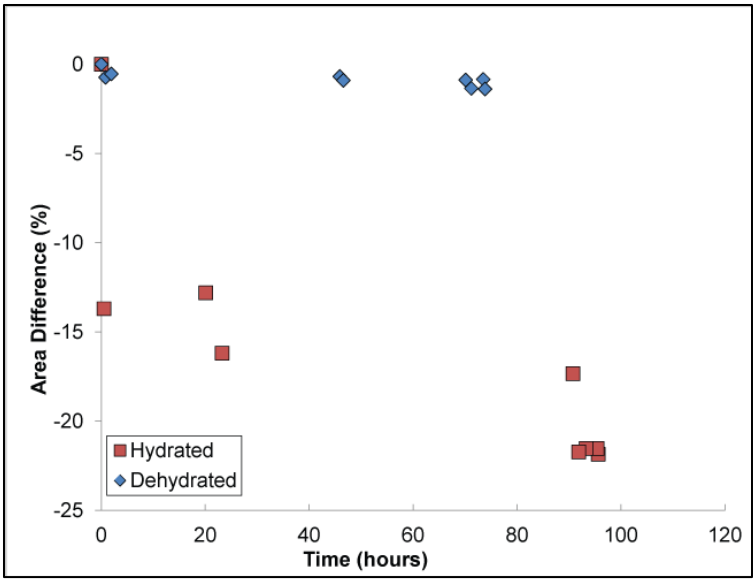

Figure 17: Comparison of the peak area corresponding to nonstructural (interlayer) water (3400 cm^{-1}) in hydrated and dehydrated montmorillonite as a function of exposure time at ~600 psi CO_2. The hydrated sample shows a significant decrease in the area of the nonstructural water peak, indicating that exposure to CO_2 gas produces a dehydrating effect. The dehydrated sample shows relatively no change in peak area as a function of CO_2 exposure time.

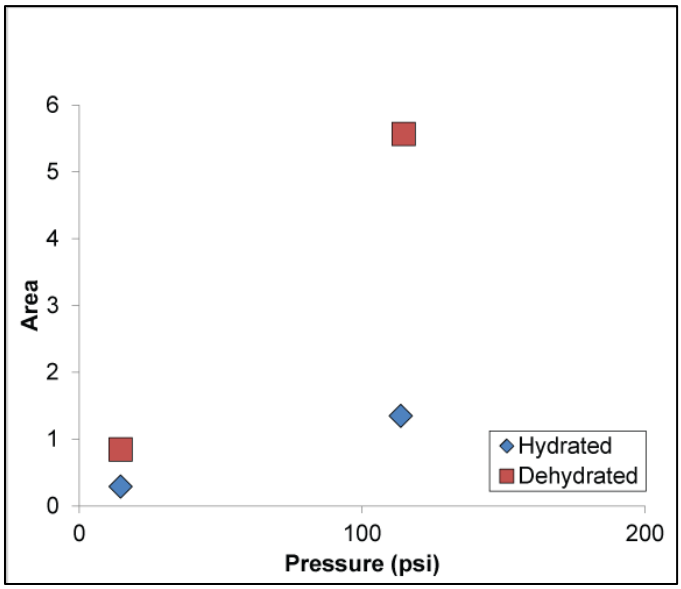

Figure 18: Comparison of the area of the v_3 CO_2 peak under ~100 psi CO_2 pressure, and the area of this same peak after the pressure had been dropped to ~1 bar. Some residual CO_2 remains in the sample after de-pressurization, as evidenced by a measureable v_3 CO_2 band in the sample. Although the dehydrated sample is able to incorporate more CO_2 than the hydrated sample, as evidenced by the larger peak area for the dehydrated sample, the peak area is similar in both the dehydrated and hydrated samples after pressure is reduced to atmospheric, indicating comparable CO_2 capacities.

significant amount of CO_2 would remain sequestered within the montmorillonite even if pressure conditions were reduced to atmospheric.

5. SUMMARY

This study examined interactions between CO_2 and Na-montmorillonite at 35° and 50°C and from ~0 - 1000 psi. Hydrated (as-received sample containing non-structural H_2O in the interlayer space), dehydrated, and re-hydrated montmorillonite were examined. Upon exposure to Na-montmorillonite, the CO_2 enters the interlayer space of the clay. This is evidenced by the v_3 CO_2 peak still present after subtracting the background spectrum of pure CO_2 gas. In the hydrated sample, as CO_2 exposure time increased, there was a decrease in the H-O-H stretching peak associated with dehydration of sample. This dehydration effect has been well documented, but does not completely dehydrate the sample of the interlayer water (Schaef et al., 2012). This behavior is interpreted to reflect the gradual displacement of nonstructural H_2O from the interlayer space with time by CO_2 entering the interlayer. When CO_2 pressure is reduced to atmospheric pressure, residual CO_2 remains in the sample. This suggests that if the seal is breached following injection of CO_2 into the reservoir, not all of the CO_2 would migrate upwards, but some would remain sequestered in the interlayer of montmorillonite.

REFERENCES

Benson, S. M., and Cole, D. R., 2008, CO(2) Sequestration in Deep Sedimentary Formations: Elements, v. 4, no. 5, p. 325-331.

Bishop, J., Madejova, J., Komadel, P., and Froschl, H., 2001, The influence of structural Fe, Al and Mg on the infrared OH bands in spectra of dioctahedral smectites: Clay Minerals, v. 37, no. 4, p. 607-616.

Bishop, J. L., Pieters, C. M., and Edwards, J. O., 1994, INFRARED SPECTROSCOPIC ANALYSES ON THE NATURE OF WATER IN MONTMORILLONITE: Clays and Clay Minerals, v. 42, no. 6, p. 702-716.

Botan, A., Rotenberg, B., Marry, V., Turq, P., and Noetinger, B. t., 2010, Carbon Dioxide in Montmorillonite Clay Hydrates: Thermodynamics, Structure, and Transport from Molecular Simulation: The Journal of Physical Chemistry C, v. 114, no. 35, p. 14962-14969.

Busch, A., Alles, S., Gensterblum, Y., Prinz, D., Dewhurst, D. N., Raven, M. D., Stanjek, H., and Krooss, B. M., 2008, Carbon dioxide storage potential of shales: International Journal of Greenhouse Gas Control, v. 2, no. 3, p. 297-308.

Cygan, R. T., Romanov, V. N., and Myshakin, E. M., 2010, Natural Materials for Carbon Capture: Sandia National Laboratories.

Cygan, R. T., Romanov, V. N., and Myshakin, E. M., 2012, Molecular Simulation of Carbon Dioxide Capture by Montmorillonite Using an Accurate and Flexible Force Field: The Journal of Physical Chemistry C, v. 116, no. 24, p. 13079-13091.

De Caritat, P., Bloch, J., Hutcheon, I., Longstaffe, F. J., and Abercrombie, H. J., 1997, Comparison of the Mineralogical and Chemical Composition of 2 Shales from the Western Canada Sedimentary Basin and the United States Gulf Coast: Clays and Clay Minerals, v. 45, no. 3, p. 327-332.

De Pablo, L., Chavez, M. L., and Monsalvo, R., 2007, The state of hydration of Ca-exchanged montmorillonite at a depth of 2-2.7 kilometers: Canadian Mineralogist, v. 45, p. 281-292.

Farmer, V. C., 1974, The Infrared Spectra of Minerals, London Mineralogical Society, 427 p.:

Flichy, N. M. B., Kazarian, S. G., Lawrence, C. J., and Briscoe, B. J., 2001, An ATR−IR Study of Poly (Dimethylsiloxane) under High-Pressure Carbon Dioxide: Simultaneous Measurement of Sorption and Swelling: The Journal of Physical Chemistry B, v. 106, no. 4, p. 754-759.

Fripiat, J. J., Cruz, M. I., Bohor, B. F., and Thomas, J., Jr., 1974, Interlamellar adsorption of carbon dioxide by smectites: Clays and Clay Minerals, v. 22, no. 1, p. 23-30.

Giesting, P., Guggenheim, S., Koster van Groos, A. F., and Busch, A., 2012, Interaction of carbon dioxide with Na-exchanged montmorillonite at pressures to 640 bars: Implications for CO2 sequestration: International Journal of Greenhouse Gas Control, v. 8, no. 0, p. 73-81.

Goodman, A. L., 2009, A Comparison Study of Carbon Dioxide Adsorption on Polydimethylsiloxane, Silica Gel, and Illinois No. 6 Coal Using in Situ Infrared Spectroscopy: Energy & Fuels, v. 23, no. 2, p. 1101-1106.

Greenwald, J., 2012, Putting the "U" in CCUS, Volume 2012: Center for Climate and Energy Solutions, Center for Climate and Energy Solutions.

Grim, R. E., 1962, Applied Clay Mineralogy: New York, McGraw-Hill, p. 422.

Gu, C., Liu, C., Johnston, C. T., Teppen, B. J., Li, H., and Boyd, S. A., 2011, Pentachlorophenol Radical Cations Generated on Fe(III)-Montmorillonite Initiate Octachlorodibenzo-p-dioxin Formation in Clays: Density Functional Theory and Fourier Transform Infrared Studies: Environmental Science & Technology, v. 45, no. 4, p. 1399-1406.

Günzler, H., and Heise, H. M., 2002, IR spectroscopy : an introduction, Weinheim, Wiley-VCH.

Herzog, H., 2001, What future for carbon capture and sequestration?: Environmental Science & Technology, v. 35, no. 7, p. 148A-153A.

IPCC, 2005, Carbon Dioxide Capture and Storage.

-, 2012, Managing the Risks of Extreme Events and Disasters to Advance Climate Change Adaptation.
Klein, C., 2001, Manual of Mineral Science, John Wiley & Sons, Inc. .
Lee, S. M., and Tiwari, D., 2012, Organo and inorgano-organo-modified clays in the remediation of aqueous solutions: An overview: Applied Clay Science, v. 59–60, no. 0, p. 84-102.
Loring, J. S., Schaef, H. T., Turcu, R. V. F., Thompson, C. J., Miller, Q. R. S., Martin, P. F., Hu, J. Z., Hoyt, D. W., Qafoku, O., Ilton, E. S., Felmy, A. R., and Rosso, K. M., 2012, In Situ Molecular Spectroscopic Evidence for CO2 Intercalation into Montmorillonite in Supercritical Carbon Dioxide: Langmuir, v. 28, no. 18, p. 7125-7128.
Madejova, J., and Komadel, P., 2005, Information available from infrared spectra of the fine fractions of bentonites, *in* Kloprogge, J. T., ed., The Application of Vibrational Spectroscopy to Clay Minerals and Layered Double Hydroxides, Volume 13: Aurora, CO, The Clay Minerals Society, p. 65-98.
McConnell, C., 2012, Adding “Utilization” to Carbon Capture and Storage: Energy.gov, U.S. Department of Energy, p. 1.
Murray, H. H., 2007, Applied Clay Mineralogy, Volume 2: Occurrences, Processing and Applications of Kaolins, Bentonites, Palygorskitesepiolite, and Common Clays, Volume 2, Elsevier Science, p. 188.
Nisbet, E. G., and Sleep, N. H., 2001, The habitat and nature of early life: Nature, v. 409, no. 6823, p. 1083-1091.
Patz, J. A., Epstein, P. R., Burke, T. A., and Balbus, J. M., 1996, Global climate change and emerging infectious diseases: Jama-Journal of the American Medical Association, v. 275, no. 3, p. 217-223.
Rother, G., Ilton, E. S., Wallacher, D., Hauβ, T., Schaef, H. T., Qafoku, O., Rosso, K. M., Felmy, A. R., Krukowski, E. G., Stack, A. G., Grimm, N., and Bodnar, R. J., 2012, CO2 Sorption to Subsingle Hydration Layer Montmorillonite Clay Studied by Excess Sorption and Neutron Diffraction Measurements: Environmental Science & Technology.
Schaef, H. T., Ilton, E. S., Qafoku, O., Martin, P. F., Felmy, A. R., and Rosso, K. M., 2012, In situ XRD study of Ca2+ saturated montmorillonite (STX-1) exposed to anhydrous and wet supercritical carbon dioxide: International Journal of Greenhouse Gas Control, v. 6, no. 0, p. 220-229.
Shaw, D. B., and Weaver, C. E., 1965, The Mineralogical Composition of Shales: Journal of Sedimentary Petrology, v. 35, no. 1, p. 213-222.
Shimanouchi, T., 1977, TABLES OF MOLECULAR VIBRATIONAL FREQUENCIES CONSOLIDATED VOLUME 2: Journal of physical and chemical reference data, v. 6, no. 3, p. 993-1102.
Sposito, G., Prost, R., and Gaultier, J. P., 1983, INFRARED SPECTROSCOPIC STUDY OF ADSORBED WATER ON REDUCED-CHARGE NA-LI-MONTMORILLONITES: Clays and Clay Minerals, v. 31, no. 1, p. 9-16.
Steele-MacInnis, M., Capobianco, R. M., Dilmore, R., Goodman, A., Guthrie, G., Rimstidt, J. D., and Bodnar, R. J., 2012, Volumetrics of CO2 Storage in Deep Saline Formations: Environmental Science & Technology.
Stevens, J. J., and Anderson, S. J., 1996, Orientation of Trimethylphenylammonium (TMPA) on Wyoming Montmorillonite: Implications for Sorption of Aromatic Compounds: Clays and Clay Minerals, v. 44, no. 1, p. 132-141.
Suekane, T., Nobuso, T., Hirai, S., and Kiyota, M., 2008, Geological storage of carbon dioxide by residual gas and solubility trapping: International Journal of Greenhouse Gas Control, v. 2, no. 1, p. 58-64.
Tzavalas, S., and Gregoriou, V. G., 2009, Infrared spectroscopy as a tool to monitor the extent of intercalation and exfoliation in polymer clay nanocomposites: Vibrational Spectroscopy, v. 51, no. 1, p. 39-43.
Van Olphen, H., and Fripiat, J. J., 1979, Data handbook for clay minerals and other non-metallic minerals, Pergamon Press, p. 346.

Yamada, H., Nakazawa, H., Hashizume, H., Shimomura, S., and Watanabe, T., 1994, Hydration Behavior of Na-Smectite Crystals Synthesized at High Pressure and High Temperature: Clays and Clay Minerals, v. 42, no. 1, p. 77-80.

Appendix A: Notebook Pages

Begin Mont. + CO_2 at 35°C

1-5-2012

Background

blank	12JA0501 (35)	$\rho^2\rho$=4.19	T=35°C	P=0 psig
Mont	12JA0502 (35)	=3.82	"	"

10:30 Add 64 psig CO_2

blank	12 Ja 05, 35, 03	$\rho^2\rho$= ~~3.84~~ 4.25	T=35°C	P=64 psig
10:45 mont.	12 Ja 05, 35, 04	$\rho^2\rho$ = 3.84	"	"

12:50 - 64 psig CO_2

blank	12JA05, 35, 05A	$\rho^2\rho$ = 4.17	T=35°C	P=64 psig
Mont	12JA05, 35, 06A	$\rho^2\rho$ = 3.84		

2:25

blank	12JA05, 35, 07A	$\rho\rho$= 4.28	T=35C	P=64 psig
mont	12JA05, 35, 08A	$\rho^2\rho$ = 3.86	T=35°C	P=64 psig

increase to ~250 psig

3:09

blank	12JA05, 35, 09A	$\rho^2\rho$= 4.24	T=35°C	P=241 psig
mont.clay	12JA05, 35, 10A	$\rho^2\rho$= 3.81	T="	P=242 psig

3:45

mont.clay	12JA05, 35, 12A	$\rho^2\rho$ = 3.77	T=35°C	P=438 psig
blank	12JA05, 35, 11A	$\rho^2\rho$ = 4.22	"	P="

bath quit recirculating overnight, temp went down to 25°C reheated in morning to 35°C.

Begin Mont. + CO_2 at 35°C

1-5-2012

Background

blank 12JA0501 (35) p^2p = 4.19 T = 35°C P = 0 psig

Mont 12JA0502 (35) = 3.82 " "

10:30 Add 64 psig CO_2

blank 12 Ja 05, 35, 03 p^2p = ~~3.84~~ 4.25 T = ~~30~~ 35°C P = 64 psig

10:45 mont. 12 Ja 05, 35, 04 p^2p = 3.84 " "

12:50 - 64 psig CO_2 -

blank 12JA05, 35, 05A p^2p = 4.17 T = 35°C P = 64 psig

Mont 12JA05, 35, 06A p^2p = 3.84

2:25

blank 12JA05, 35, 07A p^2p = 4.28 T = 35°C P = 64 psig

mont 12JA05, 35, 08A p^2p = 3.86 T = 35°C P = 64 psig

increase to ~250 psig

3:09

blank 12JA05, 35, 09A ~~p^2p~~ = p^2p = 4.24 T = 35°C P = 241 psig

mont.clay 12JA05, 35, 10A p^2p = 3.81 T = " P = 242 psig

3:45

mont.clay 12JA05, 35, 12A p^2p = 3.77 T = 35°C P = 438 psig

blank 12JA05, 35, 11A p^2p = 4.22 " P = "

bath quit recirculating overnight, temp. went down to 25°C reheated in morning to 35°C.

Ni(pXdAM)Ni(CN)4, T = -0.13 oC

increase P ~ every 15 min.

1/6/12 9:50

blank 12JA 06, 35, 01A p^2p = 4.23 P = 432 psig T = 34°C

mont. clay 12JA 06, 35, 02A p^2p = 3.76 P = 433 psig T = 34°C

10:30

blank 12 JA 06, 35, 03A p^2p = 4.26 P = 629 T = 35°C

mont. clay 12 JA 06, 35, 04A p^2p = 3.79 P = 630 T = 35°C

12:00 pm

blank 12JA06, 35, 05A p^2p = 4.25 P = 822 psig T = 35°C

mont clay 12JA06, 35, 06A p^2p = ~~3.74~~ 3.83 P = 821 psig T = 35°C

1:00 pm

blank 12JA06, 35, 07A p^2p = 4.21 P = 1056 psig T = 35°C

mont 12JA 06, 35, 08A p^2p = 3.81 P = 1053 psig T = 35°C

2:33 pm

blank 12JA06, 35, 09A } off scale p^2p = 3.99 P = 1265 psig T = 35°C

mont 12JA06, 35, 10A } p^2p = 3.81 P = 1264 psig T = 35°C

3:11 pm

blank 12JA06, 35, 11A p^2p = 4.12 P = 639 psig T = 35°C

mont 12JA06, 35, 12A p^2p = 3.82 P = 639 psig T = 35°C

3:35 pm

blank 12JA 06, 35, 13A p^2p = 3.81 P = 639 T = 35°C

Mont 12JA 06, 35, 14A p^2p = 4.11 P = 639 T = 35°C

Increase to 50°C at 641 psig CO_2

1/9/12 9:30am

blank ~~clay~~	12JA09,50,01A	$p^2p = 4.21$	P = 646 psig	T = 50°C
mont.	12JA09,50,02A	$p^2p = 3.70$	P = 646 psig	T = 50°C

10:26 decrease P to ~250 psig

blank	12JA09,50,03A	$p^2p = 4.29$	P = 250 psig	T = 50°C
clay	12JA09,50,04A	$p^2p = 3.93$	P = 251 psig	T = 50°C

11:00 decrease P to ~0 psig

blank	12JA09,50,05A	$p^2p = 4.26$	P = 1 psig	T = 50°C
clay	12JA09,50,06A	$p^2p = 3.97$	P = 1 psig	T = 50°C

11:40 Add N_2 to eliminate CO_2

blank	12JA09,50,07A	$p^2p = 4.20$	P = 254 psig	T = 50°C
mont.	12JA09,50,08A	$p^2p = 3.99$	P = 254 psig	T = 50°C

1:40

blank	12JA09,50,09A (11)	$p^2p = 4.24$	P = 1 psig	T = 50°C
mont.	12JA09,50,10A (12)	$p^2p = 4.02$	P = 1 psig	T = 50°C

4:08 ~~2:46~~ cleaned blank crystal

blank	12JA09,~~50~~,11A	$p^2p =$ ~~4.43~~ 3.76	P = ~~60~~ psig	T = ~~50~~ 21°C
mont.	12JA09,~~50~~,12A	$p^2p =$ ~~4.08~~ 3.82	P = ~~60~~ psig	T = ~~50~~°C

↑ 15 scans

open to atmosphere

crystal cleaned

Ni(pXdAM)Ni(CN)4, T = -0.13 oC

Increase to 50°C at 641 psig CO_2

1/9/12 9:30am

blank 12JA09,50,01A p^2p = 4.21 P = 646 psig T = 50°C
mont. 12JA09,50,02A p^2p = 3.70 P = 646 psig T = 50°C

10:26 decrease P to ~250 psig

blank 12JA09,50,03A p^2p = 4.29 P = 250 psig T = 50°C
clay 12JA09,50,04A p^2p = 3.93 P = 251 psig T = 50°C

11:00 decrease P to ~0 psig

blank 12JA09,50,05A p^2p = 4.26 P = 1 psig T = 50°C
clay 12JA09,50,06A p^2p = 3.97 P = 1 psig T = 50°C

11:40 Add N_2 to eliminate CO_2

blank 12JA09,50,07A p^2p = 4.20 P = 254 psig T = 50°C
mont. 12JA09,50,08A p^2p = 3.99 P = 254 psig T = 50°C

1:40

blank 12JA09,50,09A (11) p^2p = 4.24 P = 1 psig T = 50°C
mont. 12JA09,50,10A (12) p^2p = 4.02 P = 1 psig T = 50°C

4:08 ~~2:46~~ cleaned blank crystal

blank 12JA09,~~50~~,11A p^2p = ~~4.43~~ 3.76 P = ~~60~~ psig T = ~~50~~°C
mont. 12JA09,~~50~~,12A p^2p = ~~4.08~~ 3.82 P = ~~60~~ psig T = ~~50~~°C

open to atmosphere 21°

↑ 15 scans

crystal cleaned

1/10/12 Dehydrated clay - more OH than we want
dehydrate more

9:15

blank 12JA10,~~35~~ 100,01A p^2p = 4.01 P = 254 psig T = 94°C
mont. 12JA10,100,02A p^2p = 4.13 P = 254 psig T = 95°C

10:34 check to see OH² bands

blank 12JA10,100,03A p^2p = 4.04 P = 253 psig T = 98°C
mont 12JA10,100,04A p^2p = 4.19 P = 253 psig T = 98°C

1:05 no CO_2 in sample + sample is dehydrated

blank 12JA10,35,05A p^2p = 3.~~76~~ 81 P = 1 psig T = 34°C
mont. 12JA10,35,06A p^2p = 4.10 P = 1 psig T = 35°C

add CO_2 to dehydrated sample

1:30pm

blank 12JA10,35,07A p^2p = 3.87 P = 55 psig T = 35°C
mont. 12JA10,35,08A p^2p = 4.10 P = 55 psig T = 35°C

2:05

blank 12JA10,35,09A p^2p = 3.85 P = 260 psig T = 35°C
mont. 12JA10,35,10A p^2p = 4.09 P = 259 psig T = 35°C

2:35

blank 12JA10,35,11A p^2p = 4.05 P = 452 psig T = 35°C
mont. 12JA10,35,12A p^2p = 4.06 P = 454 psig T = 35°C

3:02

blank 12JA10,35,13A p^2p = 4.01 P = 653 psig T = 35°C
mont. 12JA10,35,14A p^2p = 4.06 P = 650 psig T = 35°C

1/10/12

3:35

blank 12JA10,35,15A $p^2p = 3.93$ P = 839 psig T = 35°C
mont. 12JA10,35,16A $p^2p = 4.00$ P = 842 psig T = 35°C

4:05

blank 12JA10,35,17A $p^2p = 3.90$ P = 950 psig T = 35°C
mont. 12JA10,35,18A $p^2p = 3.97$ P = 938 psig T = 35°C

1/11/12

2:18pm N pressure 15 scans

blank 12JA11,01A $p^2p = 4.37$ P = 253 psig T = 27°C
mont. 12AA11,02A $p^2p = 3.75$ P = 253 psig T = 28°C

heat clear over night
N_2 flow

1-12-2012

Elizabeth beck to VT

9:00 heating at 70°C N_2/flow
flushed bath – went to 85°C
1:00 bath at 150°C, cell at 70°C ⇒ bath clogged again

quick scan of sample at

N_2 flow

blank 12JA1201A $p^2p = 3.90$ P = 253 T = 70°C
mont 12JA1202A $p^2p = 4.15$ P = 253 T = 70°C

1:15 – blew lines again, temp increasing rapidly
1:25 103°C
1:35 114°C

2:10 118°C w/ flowing N2

blank 12JA1203A p'p= ~~3.97~~ 4.3 P= 252 flow N2 T=118°C
Mont 12JA1204A p'p= 3.97
no change from 12JA1202A

3:10
blank 12JA1205A p'p= 4.4 P= 250 Flow T=118°C
mont 12JA1206A p'p= 3.9 P T=118°C

no changes -
Stop heating / flush w/ N2 / Store under N2

1/13/2012

pressure not holding
- orings were heated too much?
- crystal cracked?

quick scan of sample/blank

blank 12JA1301A p'p= 3.83 N2 26°C
mont 12JA1302A p'p= 3.56 P= 95 T= room

crystal appears to be ok
- retightened cell changed orings on sample
blank 12JA1303A 3.6
mont 12JA1304A 3.6
methanol present

Scan of clay at room temp

1-17-2012

N_2

blank 12Ja1701A pp = 4.3 T = 26°C

Mont 12Ja1702A pp = 3.73 T = 26°C P = 2.32

a

sample looks good

Begin N_2O/H_2O flow at room temp.

RH of Room = 38%

Begin N_2 flow at 10:40 AM

RH of flowing N_2

10:30 RH 38% Room

10:40 Begin flow of UHP N_2

10:42 RH 26% and dropping under UHP N_2 flow

10:44 RH 16.4%

11:00 RH 6.8%

11:00 Begin flow N_2/water

RH decreasing

11:12 RH = 7.0% N_2/H_2 dip tube

11:31 RH 4.6%

dip tube directly to hygrometer

12:30 RH = 46%

12:32 RH = 59%

12:35 RH 64%

11/19/20

Setting up hygrometer to rehydrate sample

Diptube to hygrometer
RH 74% w/ N_2/H_2O flow

9:07
blank 12JA19,01,A $p^2p = 3.99$ P = 0 psig T = 26°C
mont. 12JA19,02,A $p^2p = 3.83$ P = 0 psig T = 26°C

10:00 ~~blank~~ water test short scan
mont 12JA19,04,A $p^2p = 3.65$
10:30
mont 12JA19,06,A $p^2p = 3.51$
11:00
mont 12JA19,08,A $p^2p = 3.48$ 76.% relative humidity
11:13 long scan before unhooking hygrometer open (not purged)
mont 12JA19,00,A $p^2p = 3.46$ P = 0 psig T = 25°C
blank 12JA19,09,A $p^2p = 3.96$ P = 0 psig T = 25°C

~~19:55pm~~ ~~Endam~~ Setting Temp to 50°C Hydrated Isotherm
didn't take blank scan
blank 12JA19,50,01A $p^2p = 4.02$ P = 58 psig T = 50°C
mont 12JA19,50,02A $p^2p = 3.47$ P = 58 T = 51°C

Purge system again to take blank scan.

11/19/12

2:00 pm new set of CO_2 isotherm N_2

blank 12JA19,50,03A $\rho^2\rho$ = 4.15 P = 0 psig T = 50°C

mont. 12JA19,50,04A $\rho^2\rho$ = 3.53 P = 0 psig T = 50°C

2:30 pm

blank 12JA19,50,05A $\rho^2\rho$ = 4.12 P = 59 psig T = 50°C

mont 12JA19,50,06A $\rho^2\rho$ = 3.49 P = 61 psig T = 50°C

11/20/12 holding cell at ~250 psig overnight

8:30

blank 12JA20,50,01A $\rho^2\rho$ = 3.84 P = 251 psig T = 50°C

mont 12JA20,50,02A $\rho^2\rho$ = 3.50 P = 251 psig T = 50°C

9:30

blank 12JA20,50,03A $\rho^2\rho$ = 3.93 P = 444 psig T = 50°C

mont 12JA20,50,04A $\rho^2\rho$ = 3.46 P = 444 psig T = 50°C

10:00

blank 12JA20,50,05A $\rho^2\rho$ = 3.91 P = 655 psig T = 50°C

mont. 12JA20,50,06A $\rho^2\rho$ = 3.43 P = 653 psig T = 50°C

10:30

blank 12JA20,50,07A $\rho^2\rho$ = 3.95 P = 847 psig T = 50°C

mont. 12JA20,50,08A $\rho^2\rho$ = 3.46 P = 846 psig T = 50°C

11:04

blank 12JA20,50,09A $\rho^2\rho$ = 3.78 P = 1064 psig T = 50°C

mont. 12JA20,50,10A $\rho^2\rho$ = 3.42 P = 1066 psig T = 50°C

12:56

blank 12JA20,50,11A $\rho^2\rho$ = 3.70 P = 1274 psig T = 50°C

mont. 12JA20,50,12A $\rho^2\rho$ = 3.24 P = 1274 psig T = 49°C

11/20/12 depressurizing sample to ~650 psig

1:30

blank	12JA20,50,13A	$\rho^2\rho = 3.76$	P = 650 psig	T = 50°C
mont.	12JA20,50,14A	$\rho^2\rho = 3.33$	P = 649 psig	T = 50°C

Replacing CO_2 with N_2

Pressure to ~ 250

~~2:45~~ 3:00pm

blank	12JA20,50,15A	$\rho^2\rho = 3.81$	P = 251 psig	T = 51°C
mont	12JA20,50,16A	$\rho^2\rho = 3.54$	P = 251 psig	T = 51°C

3:34

blank	12JA20,50,17A	$\rho^2\rho = 3.84$	P = 1260 psig	T = 50°C
mont	12JA20,50,18A	$\rho^2\rho = 3.55$	P = 1260 psig	T = 50°C

2-2-2012 Follow-up clay experiments

1. heat 118°C in N_2, cool to room
   35°C N_2, 35°C CO_2 step up/ step down (Eachen)
   dry N_2 to remove CO_2 ⇒ time to remove CO_2
2. repeat w/ H_2O/clay

			Static	
12Fe0201	blank	$p^2p = 3.77$	$P = 1010$ psig N_2	$T = 5°C$
12Fe0202	clay	$p^2p = 3.41$	$P = 1010$	

sample is hydrated - small sorbed CO_2 peak
heat to ~100°C under N_2 flow

~~1.00 Bath from 60 to 110°C under nitrogen flow~~

need to clean blank crystal ...

~~quick scan of sample after cleaning~~
out of liquid N_2

Tomorrow

2-3-2012

Sample scans at room temp

blank 12FeO301 pp= 4.23 P= 257psig N2 T= 25°C
Mont 12FeO302 pp= 3.55 P= 257psig N2 T= 25°C
some methanol present

Begin Heating

11:00

12:30 Bath = 115°C Cell = 93°C

Quick scans

blank 12FeO303 pp= 4.0 P= 257 N2 flow T= 93°C
Mont 12FeO304 pp= 3.55

Clay is dehydrated, methanol gone

try to heat to 100°C

12:45 bath to 122°C

1:45 low on liq N2

12FeO305 P= 257 N2 flow T= 99°C

12FeO306 no change from 12FeO304

Cool to room temp under N2 flow

2-6-2012 dried Mont clay + CO_2 at 35°C

- Sample under 287 psig N_2 over weekend at room temp.
- removed N_2 to 0psig

Sum of Sump clay at room temp

blank 12Fe0601 p^2p= 4.01 P=0psig T= 25°C
Mont 12Fe0602 p^2p= 3.83

10:00 begin heating to 35°C bath at 39°C
11:20 cell at 34°C - increase bath to 40°C
bath at 40, cell at 35°C
1:30 blank 12Fe0603 p^2p= 4.14 P= 0psig T= 35°C
Mont 12Fe0604 p^2p= 3.83 P= 0psig T= 35°C

Bak ground

Add 100psig CO_2 to Mont Clay at 1:35

CO_2 psig
blank 12Fe0605 p^2p= 4.01 P= 100 T= 35°C
Mont 12Fe0606 p^2p= 3.76 P= 100 T= 35°C

2:09 increase to 300 psig CO_2 Mont clay

2:25 blank 12Fe0607 p^2p= 4.02 P= 287 T= 35°C
Mont 12Fe0608 p^2p= 3.66 P= 287 T= 35°C

increase to 600psig CO2 2:40

2:55 blank 12Fe0609 pp= 3.8 P= 600 T= 35°C
Mont 12Fe0610 pp= 3.47 P= 602 T=35°C

increase to 900psig CO2 at 3:06
blank 13 — 3.92 1078 35°C
~~blank 12Fe0611 pp= 3.93 P= — T=35°C~~
3:25 Mont 12Fe0612 pp= 3.61 P= 892 T=35°C
Mont 14 pp= 3.6 P= 1076
?

pressure increased to 1076?
(data not good) leaked from pump?

~~increased to 1300 psig at 3:35~~
3:35 decrease to 900 → subtraction not good

blank 12Fe0615 pp= 3.88 P=910 T=35°C
Mont 12Fe0616 pp= 3.53 P=911 T=35°C

4:00 increase to 1200 psig

4:15 blank 12Fe0617 pp= 3.73 P=1203 T=35°C (offscale)
Mont 12Fe0618 pp= 3.33 P=1205 T=35°C

2-7-2012

Desorb CO2

		still off scale	CO2	
blank	12Fe0701	p²p= 3.9	P= 1219 psis	T= 35°C
Mont	12Fe0702	p²p= 3.6	P= 1220	T= 35°C

10:15 Desorb to 1100 psig

		still off scale		
blank	12Fe0703	p²p= 3.77	P= 1124	T=
Mont	12Fe0704	p²p 3.5	P= 1123	T= 35°

11:00 Decrease to 1080

10:00

11:20				
blank	12Fe0705	p²p= 3.5	P= 1081	T= 35°C
Mont	12Fe0706			

1:30

12:00

blank	12Fe0707	p²p= 3.9	P= 1081	T= 35°C
Mont	12Fe0708	p²p 3.7	P= 1081	T= 35°C

Ac

12:30 decrease to 600 psis

12:45

blank	12Fe0709	p²p= 3.7	P= 600	T= 35°C
Mont	12Fe0710	p²p 3.5	P= 600	T= 35°

2:00

2:15

2-7-2012 Desorb Cor from dried Mont Clay at 35°C

2:00

blank	12Fe0711	p^2p= 3.90	P=601	T=35
Mont	12Fe0712	p^2p= 3.71	P=600	T=35°C

2-9-2012

blank	12Fe0901	p^2p= 3.92	P=58[illegible]	T=35°C
Mont	12Fe0902	p^2p= 3.76	P=[illegible]	T=35°C

10:10 decrease to 300psig

10:45	blank	12Fe0903	p^2p= 3.7	P=300	T=35°C
	Mont	12Fe0904	p^2p= 3.6	P=300	T=35°C

2-10-2012

10:00	blank	12Fe1001	p^2p=4.0	P=304	T=35°C
	Mont	12Fe1002	p^2p= 3.8	P=304	T=35°C

10:24 decrease to 100 psig

11:20	blank	12Fe1003	4.1	P=99	T=35°C
	Mont	12Fe1004	p^2p= 3.8	P=99	T=35°C

1:30

blank 12Fe 1005 p^2 4.0 CO_2 psig P=99 T=35°C

Mont 12Fe 1006 p^2p 3.8

2:00 decrease to 0 psig — NO N_2 flow

blank 12Fe 1007 3.97 psig P=0 p^2 psig

mont 12Fe 1008 p^2p=3.8 P=0 T=35°C

2-13-2012

blank

mont

blank 12Fe 1301 p^2p=3.97 P=0 psig T=35°C

mont 12Fe 1302 p^2p=3.83 P=0 T=35°C

pull vacuum, scan only sample, 50 scans = 47 secs.

12:52 Begin vacuum

12:53 Mont 12Fe 1304 p^2p=~~3.88~~ 3.91 P=-11 psig T=35°C

12:55 Mont 12Fe 1306 p^2p=3.93 P=-12 psig 35°C

12:57 Mont 12Fe 1308 p^2p=3.94 P=-13 psig 35°C

1:02 Mont 12Fe 1310 p^2p=3.94 P=-14 psig 35°C

1:12 Mont 12Fe 1312 p^2p=3.93 P=-14 35°C

1:40 250 scans

1:17 Mont 12Fe 1314 p^2p=3.91 P=-14 35°C

1:37 Mont 12Fe 1316 p^2p=3.86 P=-14 35°C

2:53 Mont 12Feb18 pp= 3.7 P=-14psig 35°C

3:40 Mont 12Feb20 pp= 3.75 P=-15 35°C

3:53 Mont 12Feb22 pp=3.6 P=15 35°C

Very small changes

- Vacuum over night

2-14-2012

9:45 AM Mont 12Feb1402 pp=3.9 P=-15 35°C

~~disconnected~~ disconnected vacuum

- pressure test at 256 psig N2 to check o-rings

- holds pressure

Quick scan under N2

N2

Mont 12Feb1401 pp=3.9

Mont 12Feb1402 pp=3.7 P=256 35°C

- Mont needs to be cleaned

2:53 Mont 12Fe1318 p^2p = 3.7 P = -14 psig 35°C

3:40 Mont 12Fe1320 p^2p = 3.75 P = -15 35°C

3:53 Mont 12Fe1322 p^2p = 3.6 P = 15 35°C

Very small changes

- vacuum over night

2-14-2012

9:45 AM Mont 12Fe1402 p^2p = 3.9 P = -15 35°C

~~disconnected~~ disconnected vacuum

- pressure test at 256 psig N_2 to check orings
- holds pressure

quick scan under N_2

N_2

Bark 12Fe1401 p^2p = 3.9

Mont 12Fe1402 p^2p = 3.7 P = 256 35°C

- Bark needs to be cleaned

2-21-2012

- changed detectors! — MCTB needs to be evacuated
- ~~changed~~ orings on sample and blank
- cleaned blank crystal
- restarted computer

Scans open to room air, both circ at 40°C

Scans = 50 34°C N2

blank	12Fe2101	pp = 5.54	T = ~~room~~	P = 250
mont	12Fe2102	pp = 5.89	T = ~~room~~ 34°C	P = 256

- changed stripped fittings on ATR cell

2:50 Begin hydrating sample at 35°C

3:10 64% RH

blank	12Fe2103	pp = 5.80	T = 35°C	P = 2	N2/H2O flow
mont	12Fe2104	pp = 5.22			

⇒ stopped heating

72% RH

no signal?

↓

cooling causing H2O vapor to sat?!

100, 380, 600, 900, 1200

2-23-2012

P at 115? leaking? 250 scans

blank 12Fe2301 p'p = 5.8 T = 35°C P = $\frac{N_2}{115}$
mont 12Fe2302 p'p = 5.6 T = 35°C P = 115 psig

Sample looks ok, less sorbed H_2O than other previous experiment

- flowing H_2O/N_2 again at 35°C

Start 10:45 AM

11:30 50 scans

75% RH blank 12Fe2303 p'p = 6.05 T = 35°C P = N_2/H_2O flow
mont 12Fe2304 p'p = 5.6 T = 35°C
- decrease in sorbed water

11:40 seal exit valve to further saturated w/ H_2O

11:50 sealed

blank 12Fe2305 p'p = 6.0 T = 35° P = 27 N_2/H_2O
mont 12Fe2306 p'p = 5.55 T = 35°C

12:00 back under N_2/H_2O flow
1:00 new at (1% RH)

trying to dry drierite again, detector has low signal again

1:50 75% RH at 35°C, detector is back

blank 12Fe2307 p'p=6.03 T=35°C 75°
mon 12Fe2308 p'p=5.50 T=35°C 75%RH
No flow

Add 100, 300, 600, 900, 1200 psig CO_2

2:00 Add 100 psig CO_2

					psig CO_2
2:15	blank	12Fe2309	p'p= 6.07	T=35°	100
	mont	12Fe2310	p'p= 5.54	T=35°	

2:30 Add 304 psig CO_2

					psig CO_2
2:45	blank	12Fe2311	p'p= 6.02	T=35°	304
	mont	12Fe2312	p'p= 5.40	T=35°	

3:00 Add 600 psig CO_2

					psig CO_2
3:15	blank	12Fe2313	p'p= 5.97	T=35°C	599
	mont	12Fe2314	p'p= 5.35	T=35°C	

Add 890 psig CO_2

					psig CO_2
3:45	blank	12Fe2315	p'p= 5.94	T= 35°	885
	mont	12Fe2316	p'p= 5.40	T= 35°	

3:40 Add 1023 psig CO_2

				psig CO_2
blank	12Fe2317	p^2p = 5.72	T = 35°C	1022
Mont	12Fe2318	p^2p = 5.40	T = 35°C	

4:00 increase to 1146

				psig CO_2
blank	12Fe2319 / offside	p^2p 5.60	T = 35°C	1152
Mont	12Fe2320	p^2p 5.15		

4:15 desorb to 600

				psig CO_2
blank	12Fe 2321	p^2p = 5.98	T = 35°C	601
Mont	12Fe 2322	p^2p = 5.41		

2-24-2012

				psig CO_2
blank	12Fe2401	p^2p = 5.81	T = 35°C	600
Mont	12Fe2402	p^2p = 5.56		

12:00 decrease to 300

				psig CO_2
1:00 blank	12Fe2403	p^2p = 5.97	T = 35°C	304
Mont	12Fe2404	p^2p = 5.4		

				psig CO_2
3:00 Mont	12Fe2406	p^2p = 5.26	T = 35°C	306

2-27-2012

blank 12Fe2701 5.63

Mont 12Fe2702 pp=5.10 P=295 T=35°C

~~[illegible]~~

10:48 decrease to 100

11:30 Mont 12Fe2704 5.20 P=100 T=35°C

1:10 Mont 12Fe2706 5.21 P=100 T=35°C

3:12 Mont 12Fe2708 ~~4.9~~ 5.10 P=100 35°C

decrease to 0 psig

Mon 12Fe2710 5.19 P=0 35°C

~~Mont 12Fe2710 5.19~~

~~Vacuum~~

2-28-2012 vacuum desorb

pressure at 1 psig - opened valve to 0 psig

Mont 12Fe2802 pp=5.2 P=0 35°C

Begin vacuum mode, Scan only sample side

50 scans

9:45	Begin Vacuum			psig	T=
50 scans 9:46	Mont	12Fe2804	pp= 5.06	P= -14	35°C
9:47	Mont	12Fe2806	pp= 5.06	P= -14	35°C
9:48	Mont	12Fe2808	pp= 5.02	P= 14	
9:55	Mont	12Fe2810	pp= 5.02	P= -14	
250 scans					
10:05	Mont	12Fe2812	pp= 5.02	P= -14	
10:45	Mont	12Fe2814	pp= 5.02	P= -14	

4962

3/19/12

loaded new sample

Hydrate to % relative humidity

loaded NaMont clay in methanol slurry

- Sample corrosive is very hissy

Set bath to 39°C → sample at 32°C

need 35°C — increased bath to 40°C

Scan of clay, NaMont under N_2

				P_{N_2} psig
blank	12Na1901	p^2p = 4.46	T = 33°C	270
NaMont	12Na1902	p^2p = 3.17	T = 35°C	

→ looks similar to 12Ja05,35,02A

prepare to hydrate NaMont

Room humidity of 67%

→ humid day

weather.com 67% RH outside

Flowing dry N_2 over clay

	RH	
1:20	67%	No flow
1:20	40%	N_2 flow
1:22	33%	N_2 flow

end

Begin N_2/H_2O flow over clay

N_2/H_2O Flow

	RH	
1:27	40%	N_2
Began flow 1:28	60.8%	N_2/H_2O
1:32	57%	N_2/H_2O out of flow?

— refilled dip tube

RH still at 57%

Scans

blank 12Na1903

NaMont 12Na1904

3/20/12 - purged all night

background scan before hydration 77.9% RH before going to sample

12ma2002	ment	p^2p = 3.60	P = 2 psig	T = 35°C
12ma2001	blank	p^2p = 5.01	P = 1 psig	T = 35°C

hydrate sample 10:35 am

started @ 55% RH

ended @ 65.1 RH

10:57 am ★ background ★

blank	12ma2003	p^2p = 5.03	P = 0 psig	T = 35°C
ment	12ma2004	p^2p = 3.44	P = 0 psig	T = 35°C

11:20 added CO_2 @ 200 psig

adsorb run

11:39

blank	12ma2005	$\rho^2 p = 5.01$	$P = 199$ psig	$T = 35°C$
mont	12ma2006	$\rho^2 p = 3.62$	$P = 199$ psig	$T = 35°C$

increase to ~400 psig

1:52 pm

blank	12ma2007	$\rho^2 p = 4.99$	$P = 402$ psig	$T = 34°C$
mont	12ma2008	$\rho^2 p = 3.49$	$P = 402$ psig	$T = 34°C$

increase to 600 psig

1:30 pm

blank	12ma2009	$\rho^2 p = 5.00$	$P = 603$ psig	$T = 35°C$
mont	12ma2010	$\rho^2 p = 3.64$	$P = 603$ psig	$T = 35°C$

increase to 800 psig

2:00 pm

blank	12ma2013	$\rho^2 p = 4.91$	$P = 798$ psig	$T = 35°C$
mont	12ma2012	$\rho^2 p = 3.60$	$P = 796$ psig	$T = 35°C$

increase to 1000 psig

2:33 pm

blank	12ma2015	$\rho^2 p = 4.84$	$P = 974$ psig	$T = 35°C$
mont	12ma2014	$\rho^2 p = 3.54$	$P = 975$ psig	$T = 35°C$

~~Desorb to 600~~

decrease to 600 psig 603

3:05 pm

blank	12ma2017	$\rho^2 p = 4.84$	$P = 597$ psig	$T = 35°C$
mont	12ma2016	$\rho^2 p = 3.53$	$P = 599$ psig	$T = 35°C$

Stay @ ~600 psig then wait 30 min.

3:52 pm

blank	12ma2019	$\rho^2 p = 4.97$	$P = 585$ psig	$T = 35°C$
mont	12ma2018	$\rho^2 p = 3.71$	$P = 583$ psig	$T = 35°C$

adsorb run

11:39
blank 12ma2005 $p^2p = 5.01$ $P = 199$ psig $T = 35°C$
mont 12ma2006 $p^2p = 3.62$ $P = 199$ psig $T = 35°C$
increase to ~400 psig

1:27 pm
blank 12ma2007 $p^2p = 4.99$ $P = 402$ psig $T = 34°C$
mont 12ma2008 $p^2p = 3.49$ $P = 402$ psig $T = 34°C$
increase to 600 psig

1:30 pm
blank 12ma2009 $p^2p = 5.00$ $P = 603$ psig $T = 35°C$
mont 12ma2010 $p^2p = 3.64$ $P = 603$ psig $T = 35°C$
increase to 800 psig

2:00 pm
blank 12ma2013 $p^2p = 4.91$ $P = 798$ psig $T = 35°C$
mont 12ma2012 $p^2p = 3.60$ $P = 796$ psig $T = 35°C$
increase to 1000 psig

2:33 pm
blank 12ma2015 $p^2p = 4.84$ $P = 974$ psig $T = 35°C$
mont 12ma2014 $p^2p = 3.54$ $P = 975$ psig $T = 35°C$.
~~Desorb to 600~~
decrease to 600 psig 603

3:05 pm
blank 12ma2017 $p^2p = 4.84$ $P = 597$ psig $T = 35°C$
mont 12ma2016 $p^2p = 3.53$ $P = 599$ psig $T = 35°C$
stay @ ~600 psig then wait 30 min.

3:52 pm
blank 12ma2019 $p^2p = 4.97$ $P = 585$ psig $T = 35°C$
mont 12ma2018 $p^2p = 3.71$ $P = 583$ psig $T = 35°C$

3/20/17

5:02 pm
blank 12ma2021 $p^2p = 5.00$ $P = 580$ psig $T = 35°C$
mont 12ma2020 $p^2p = 3.69$ $P = 580$ psig $T = 35°C$

3/21/02 Pressure on arrival 581!

~~8:37~~ am 9:15 am
blank 12ma2101 $p^2p = 4.66$ $P = 581$ psig $T = 35°C$
mont 12ma2102 $p^2p = 3.53$ $P = 581$ psig $T = 35°C$
~~10:16~~ am 10:16 am
blank 12ma2103 $p^2p = 4.83$ $P = 576$ psig $T = 35°C$
mont 12ma2104 $p^2p = 3.53$ $P = 576$ psig $T = 35°C$
11:15 am
blank 12ma2105 $p^2p = 4.88$ $P = 573$ psig $T = 35°C$
mont 12ma2106 $p^2p = 3.65$ $P = 573$ psig $T = 35°C$
12:18 pm
blank 12ma2107 $p^2p = 4.90$ $P = 571$ psig $T = 35°C$
mont 12ma2108 $p^2p = 3.61$ $P = 571$ psig $T = 35°C$
~~15~~
blank ~~$p^2p = 4.74$~~
Source died?

Appendix B: Raw and Subtracted Data

Please open the file FTIR CO2 Montmorillonite Data.xlsx to view the raw and subtracted data.